Deep learning segmentation of TEM micrographs acquired via in-situ irradiation: challenges and perspectives

Camilo A. F. Salvador, Lisa Vessier-Alary, Antoine Dartois, Thomas Bilyk, Stéphanie Jublot-Leclerc, Cédric Baumier, Brigitte Décamps, Estelle Meslin & Mihai-Cosmin Marinica

Université Paris-Saclay, CEA, Service de Recherche en Corrosion et Comportement des Matériaux, SRMP, 91191, Gif-sur-Yvette, France

IJClab, Laboratoire de Physique des 2 infinis Irène Joliot-Curie, Université Paris-Saclay, Orsay, 91400, France

Outline

Project: "Accurate identification and characterization of defects in materials enabled by deep learning image analysis", **June 2024-2027**, Cross-disciplinary initiative for digital science (*Mission Numérique*);

Today's presentation:

1) *"State of the art of machine learning in materials science electron microscopy"*, shortly on arXiv;

2) *"High-throughput analysis of dislocation loops in irradiated metals using Mask R-CNN";*
   Salvador et al., Micron 201 (2026) 103927

1) *"Dislocation loop growth in Al revealed by DL segmentation of in situ TEM videos";*
   Part of L. Vessier-Alary's thesis.

2) Conclusions, challenges and perspectives.

(1) State of the art: AI vs ML vs DL

Jim Gray. The Fourth Paradigm: Data-Intensive Scientific Discovery. Microsoft Research, October 2009; Image adapted from *Agrawal & Choudhary*, APL Materials 4, 2016

Bottom: Images adapted from *Pichler & Hartig*, Methods Ecol Evol. 14, 2023

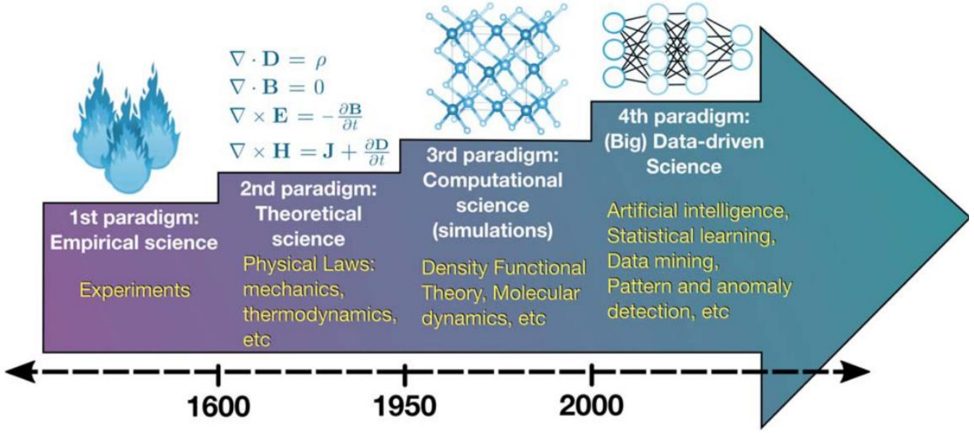

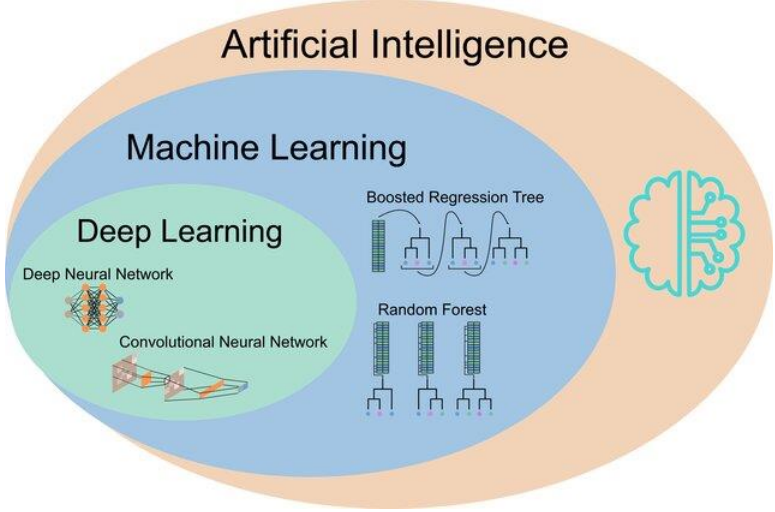

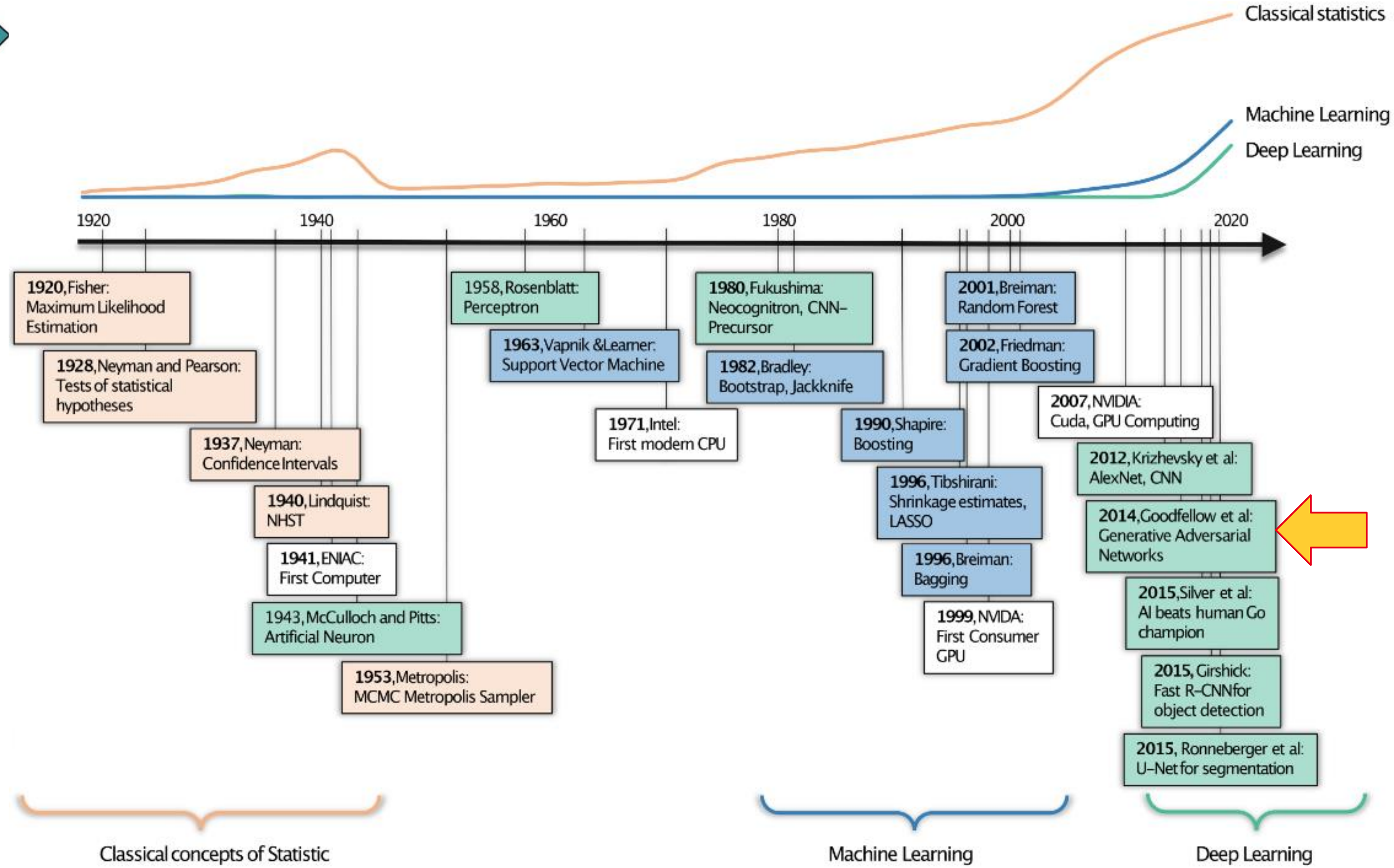

(1) State of the art: DL in materials microscopy

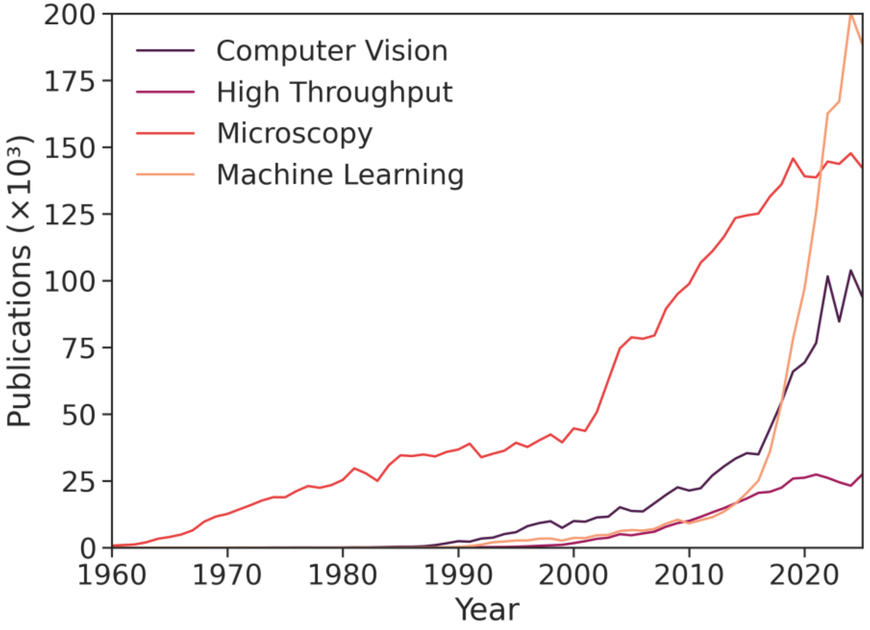

Fig. 1. Evolution of publications per year on topics such as Computer Vision, High-Throughput, Microscopy, and Machine Learning. The data were obtained from the Web of Science (all databases) in January 2026.

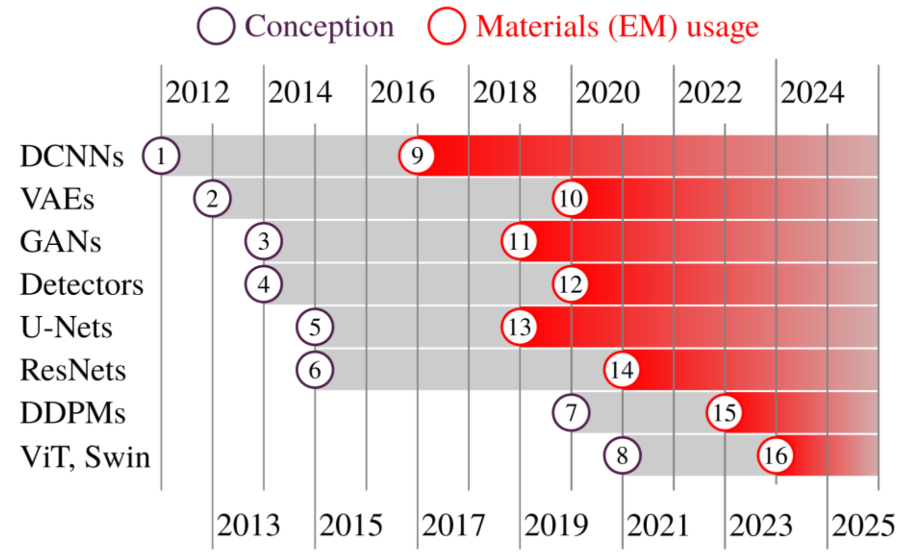

Fig. 2. Timeline of the most critical model families in computer vision and their respective adoption in materials science electron microscopy.

References:

(1) Krizhevsky et al. (2012);
(2) Kingma & Welling (2013);
(3) Goodfellow et al. (2014);
(4) Girshick et al. (2014);
(5) Ronnenberger et al. (2015);
(6) He et al. (2016);
(7) Ho et al. (2020);
(8) Dosovitskly et al. (2021);
(9) Ziatdinov et al. (2017);
(10) J. Ede (2020);
(11) de Haan et al. (2019);
(12) Okumev et al. (2020);
(13) Yao et al. (2019);
(14) Saxena et al. (2021);
(15) Azqadan et al. (2023);
(16) Qiao et al. (2024).

shortly on arXiv;

(1) Opportunities: DL in materials microscopy

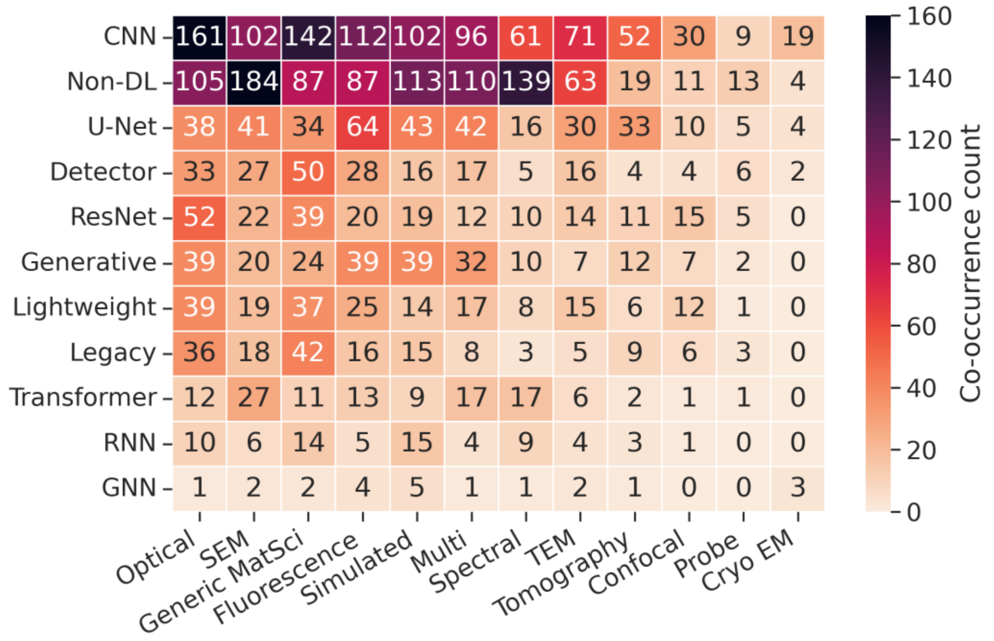

Fig. 3. Co-occurrence frequency of models and data types

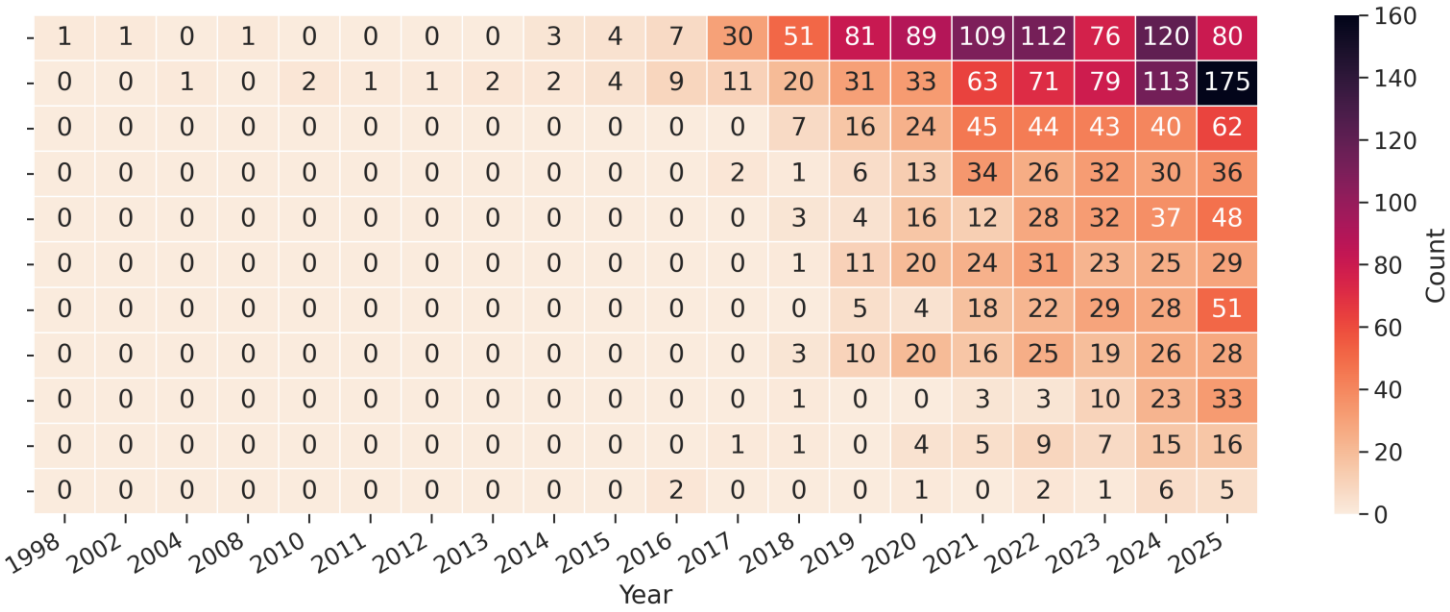

Fig. 4. Materials microscopy papers citing specific machine learning model types over the years.

shortly on arXiv;

(1 .. 2) State of the art: Computer Vision (CV)

Credits: mdpi remote sensing

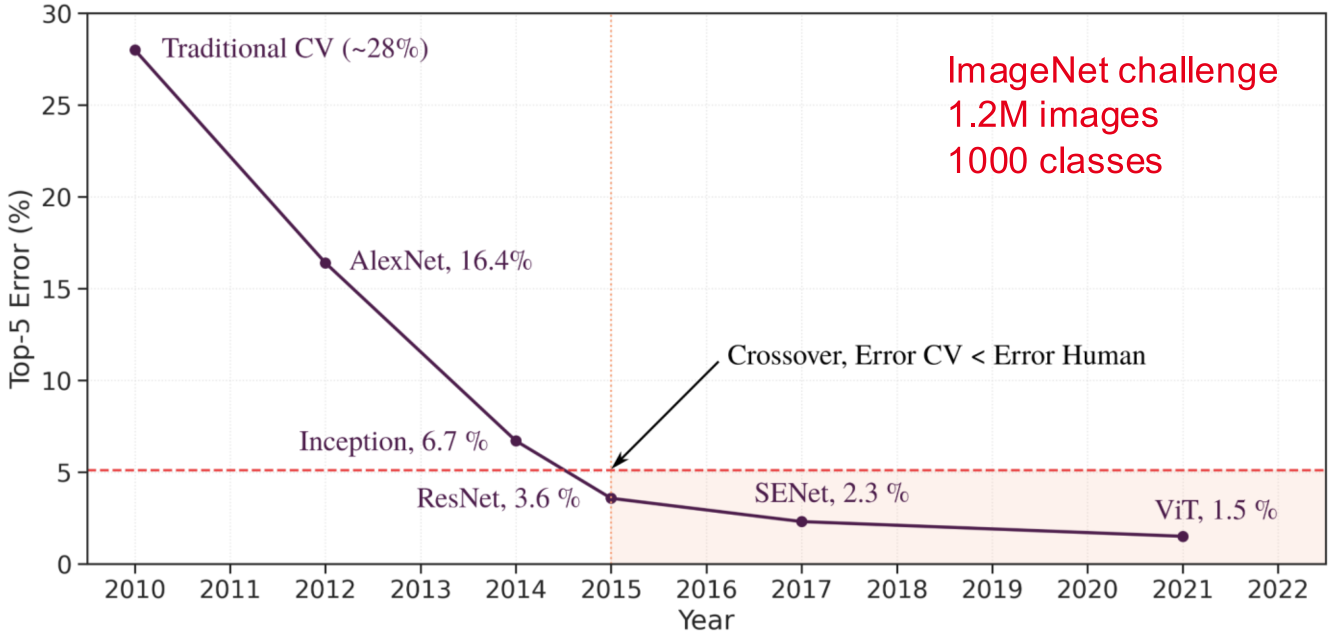

Residual connections: ResNet;
He et al., CVPR 2015.

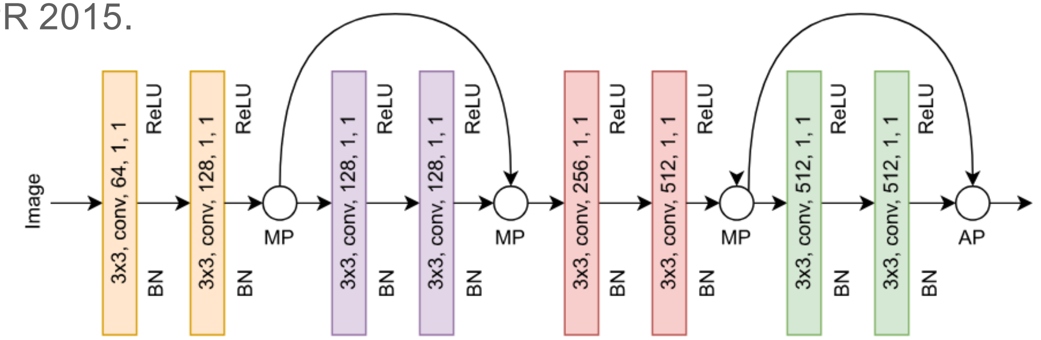

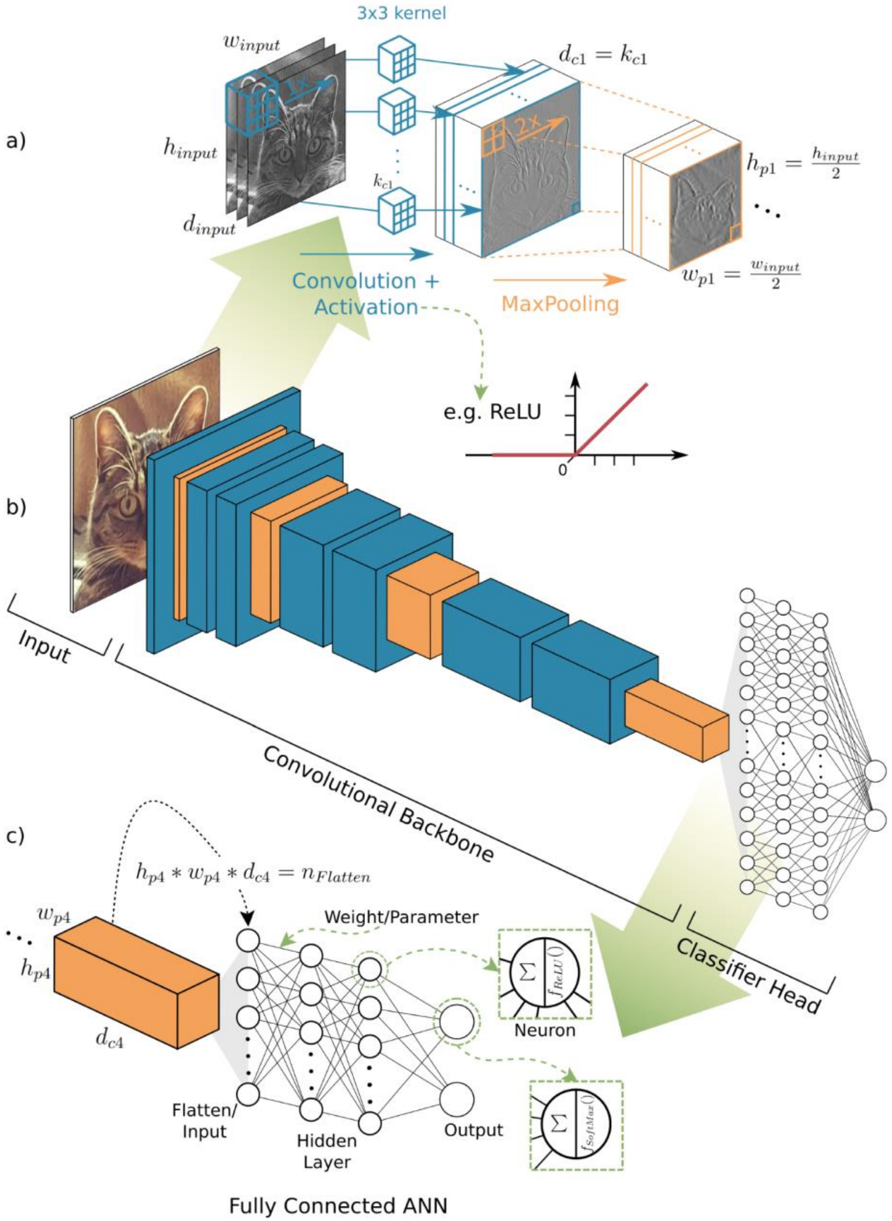

(1 .. 2) State of the art: Computer Vision (CV)

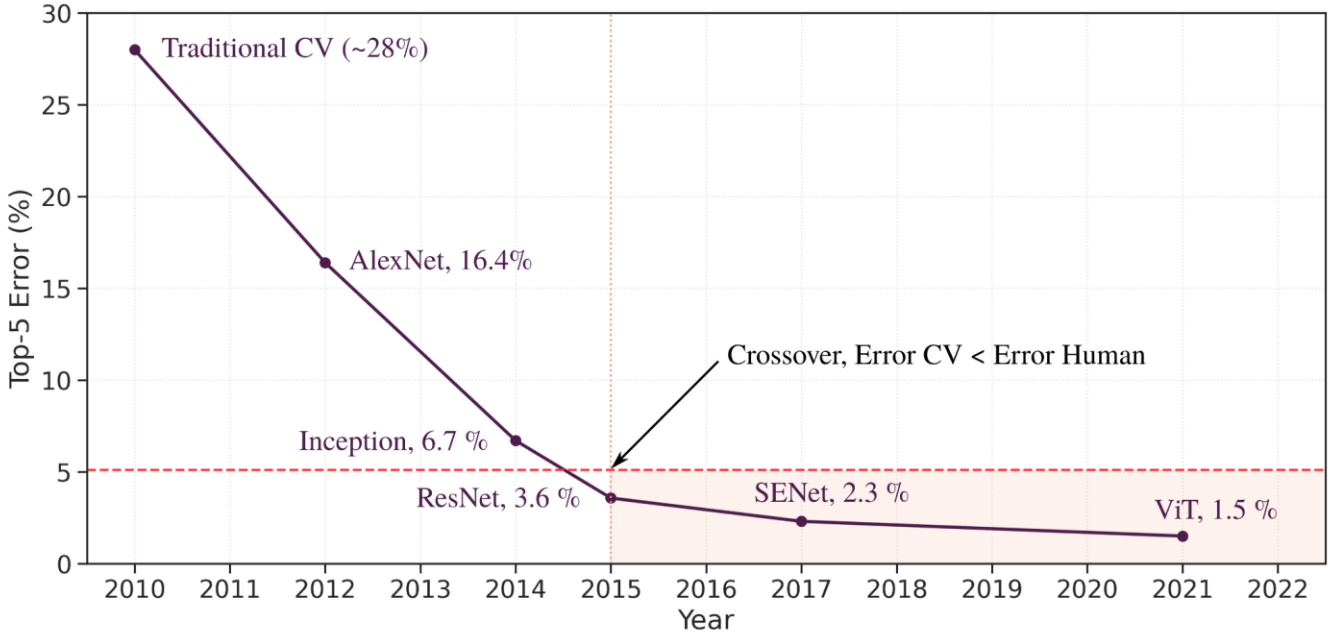

Any CNN-backbone

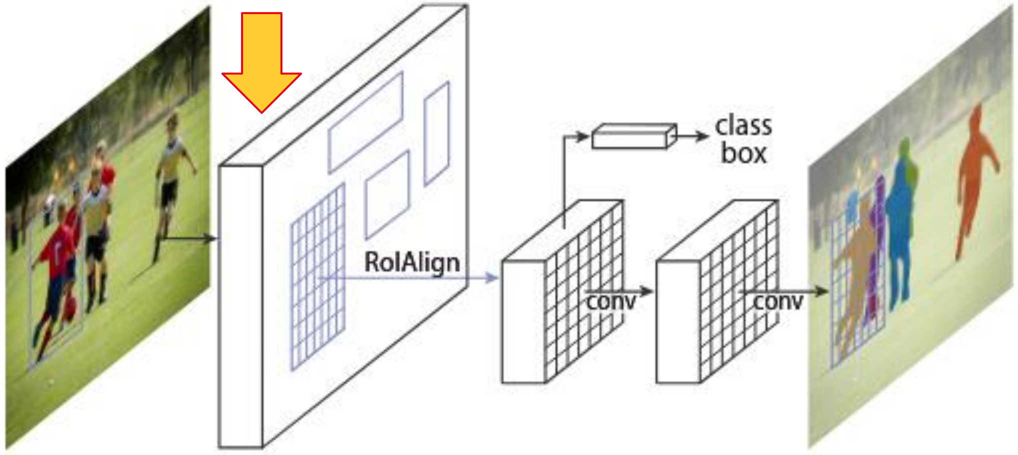

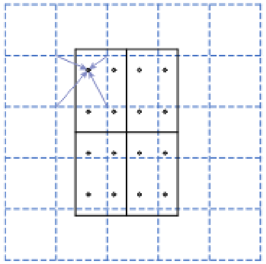

Roi Align: Mask R-CNN
He et al., CVPR 2017.
Images from the arXiv version
arXiv:1703.06870v3 [cs.CV]

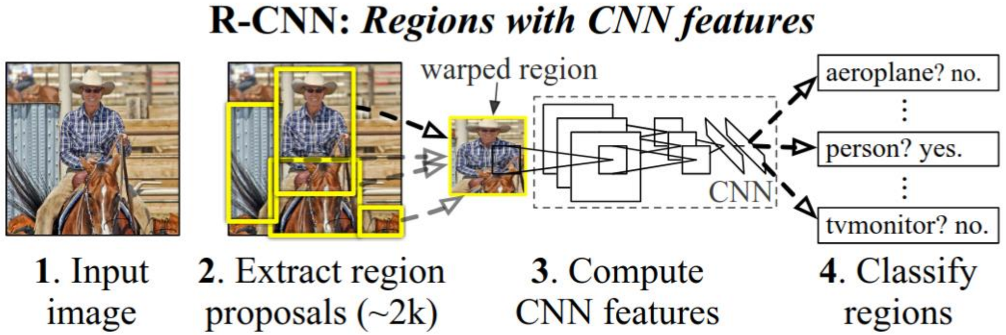

Region Proposals: R-CNN
Girshick et al., CVPR 2014.
Images from the arXiv version;
arXiv:1311.2524v5 [cs.CV]

(2) Materials under irradiation

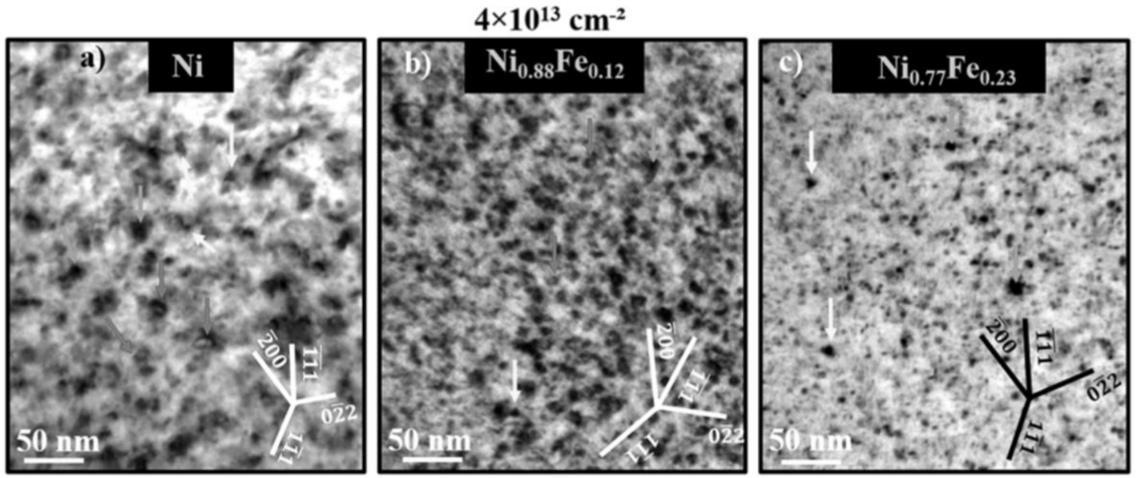

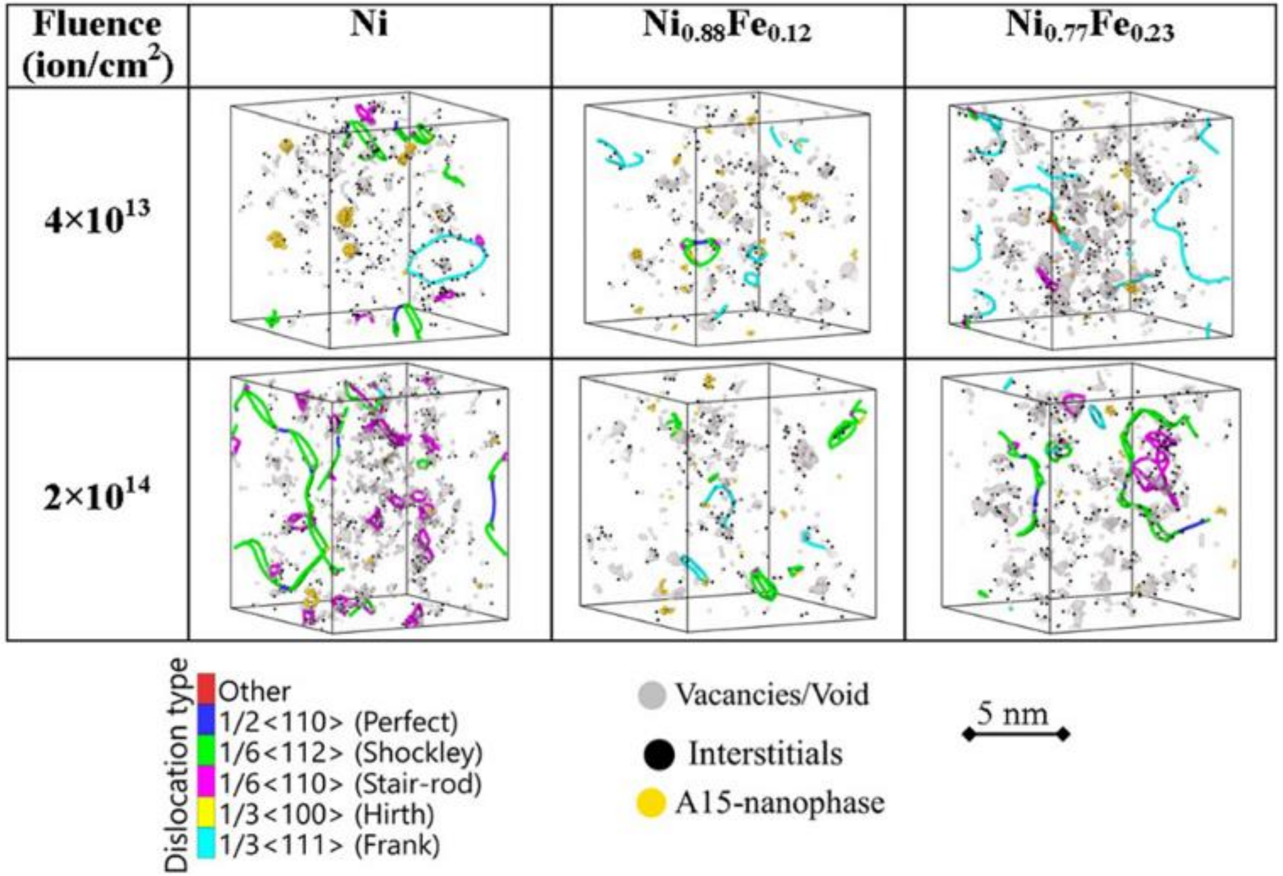

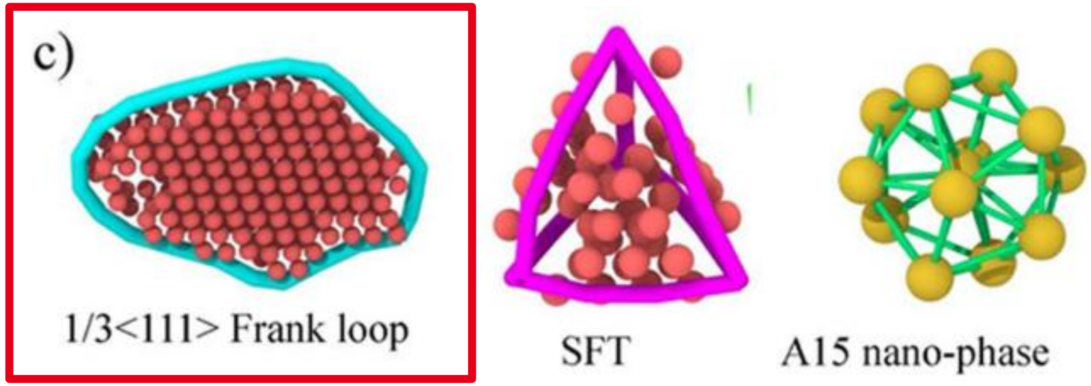

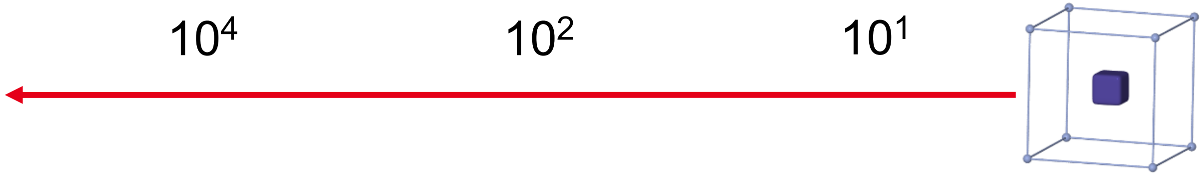

(a few images adapted from)
Wyszkowska et al., Nanoscale, 2025, 17, 15841

(2) Preliminary works at the CEA

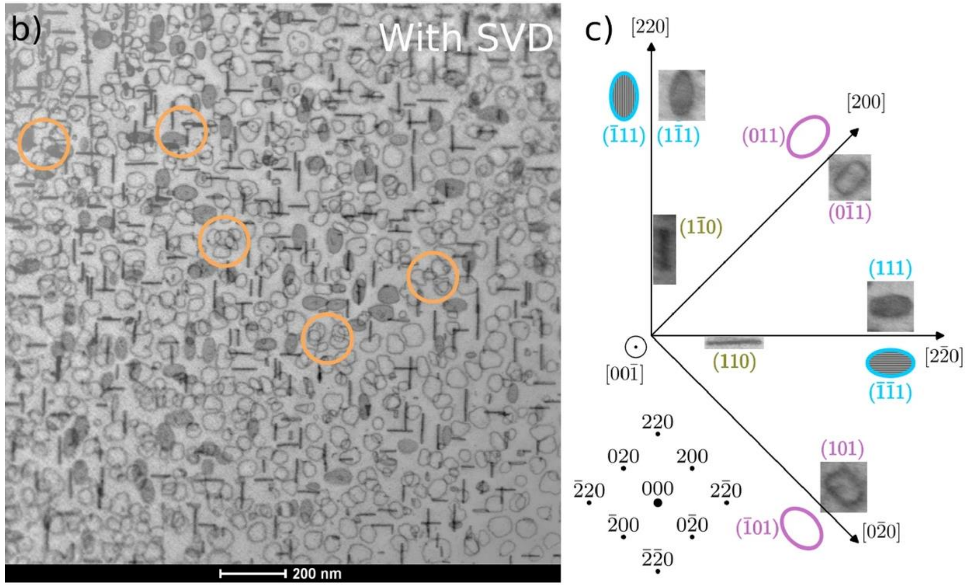

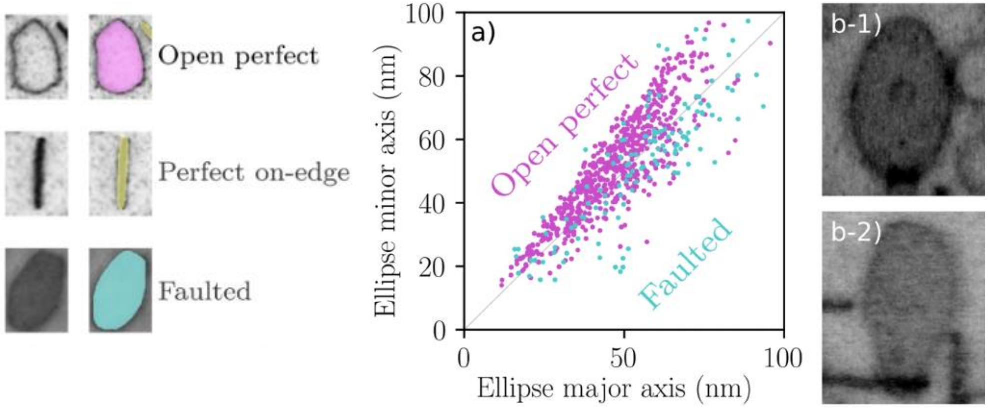

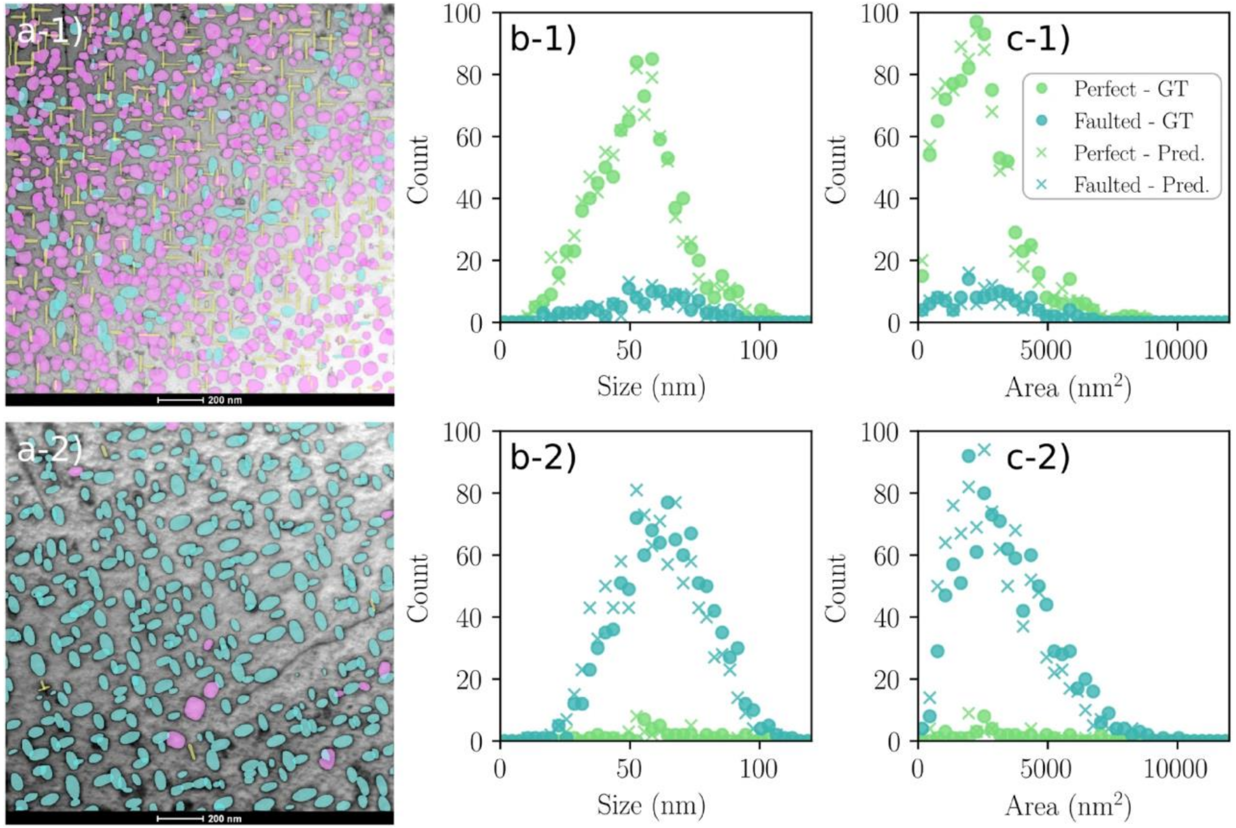

Bilyk et al., 2024
Sci. Rep. 14, 25168 (2024)

- 15Cr-46Fe-17Mn-22Ni (at.%) (Y3)
- 16Cr-37Fe-13Mn-34Ni (at.%) (ES1)
- Irradiation experiments with Fe^{+} and Ni^{2+}
- T = 550 ℃

(2) In situ irradiation experiments

JANNus-Orsay
Gentils and Cabet, 2019 Nucl. Instrum. Methods Phys. Res., Sect. B, 447 (2019)

Problem at hand: In situ platforms produce data volumes that are virtually impossible to analyze without ML (or other data analysis) algorithms.

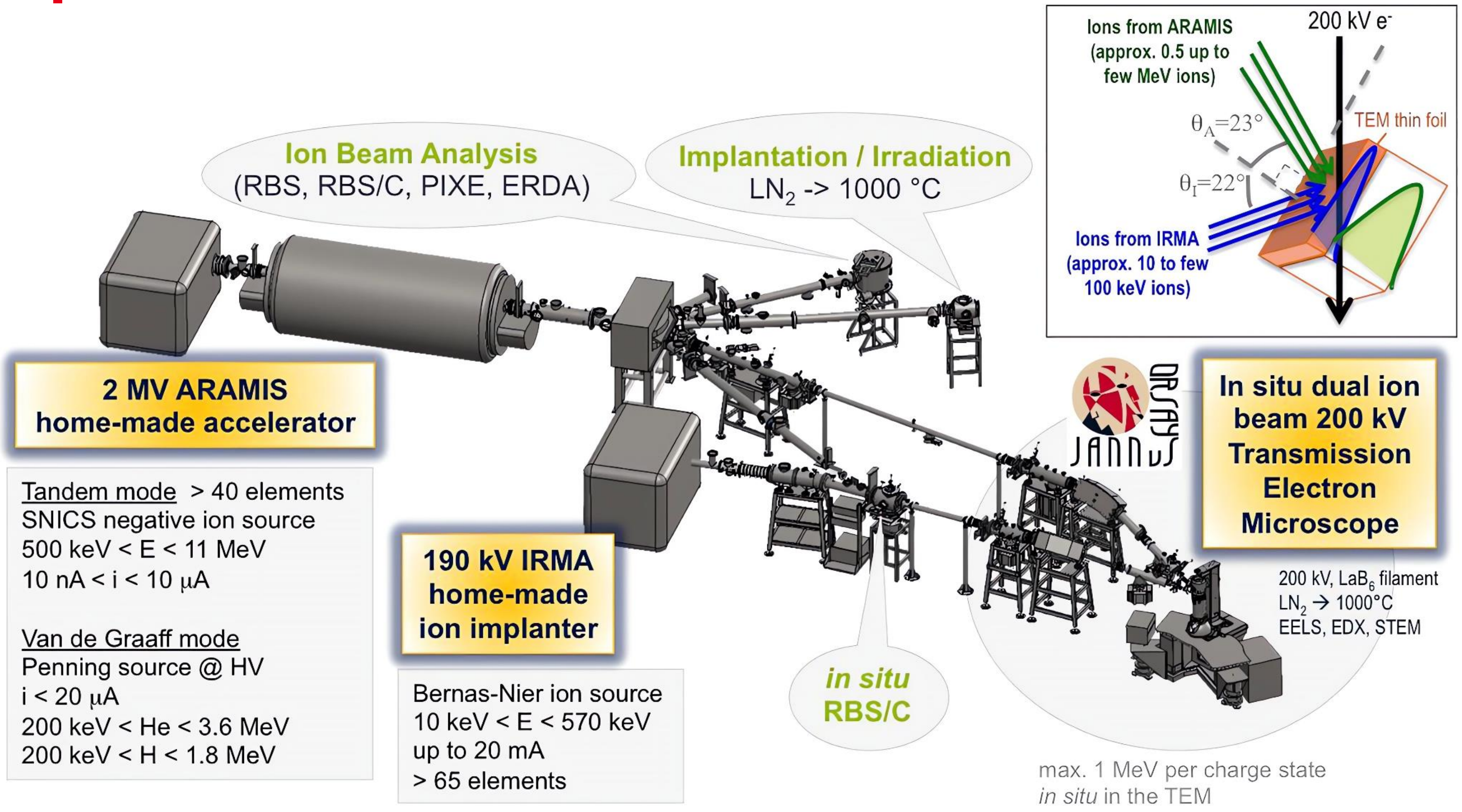

- Spatial resolution of 0.22 nm.
- **2048 x 2048 px CCD camera (up to 30 fps) -> up to 1.3 TB per hour**
- Additional wide-area imaging camera

(2) Proposed framework: github.com/ai-atoms/creme

Salvador et al., 2026
Micron 201 103927

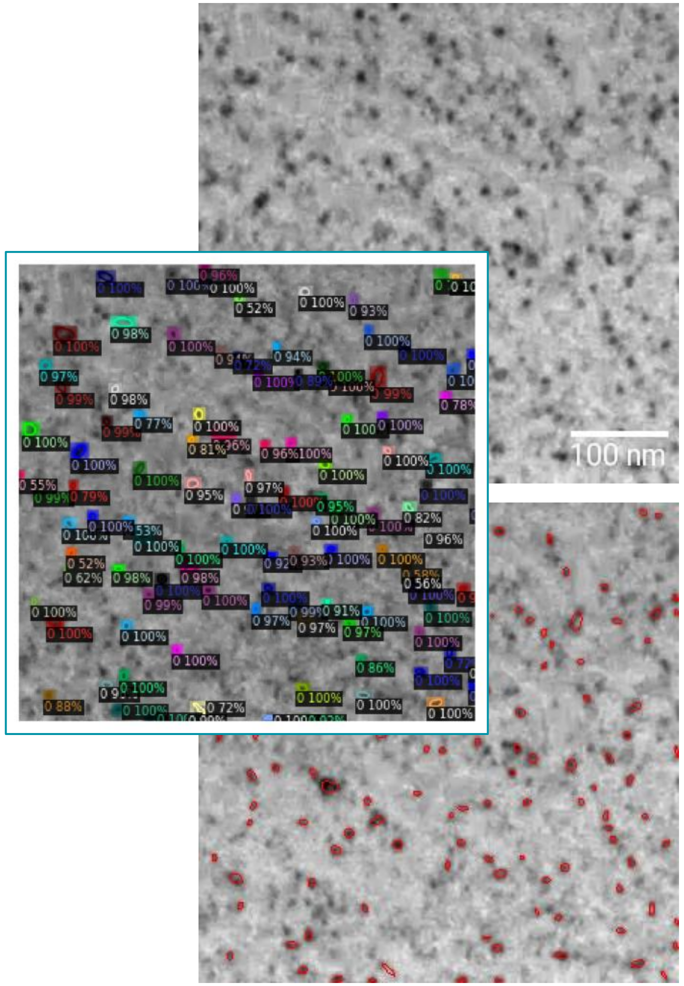

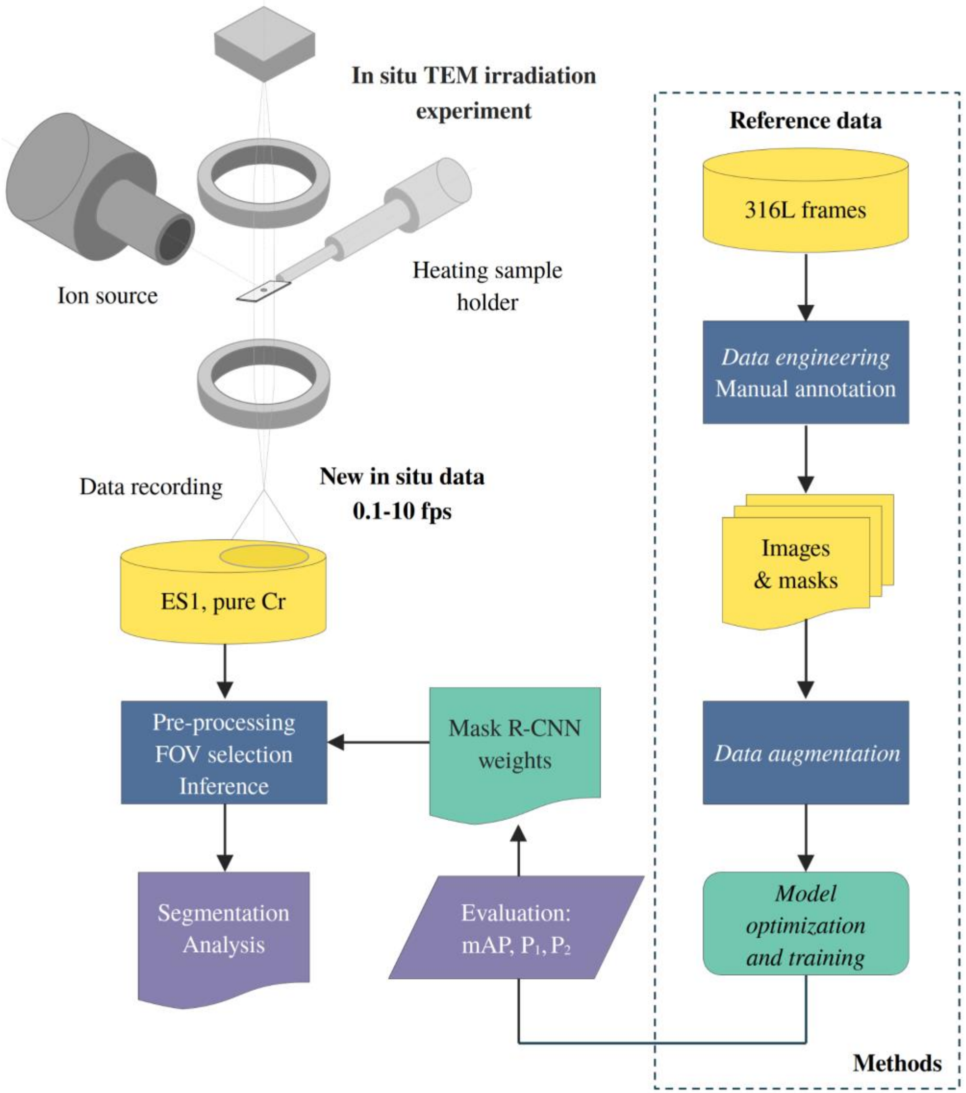

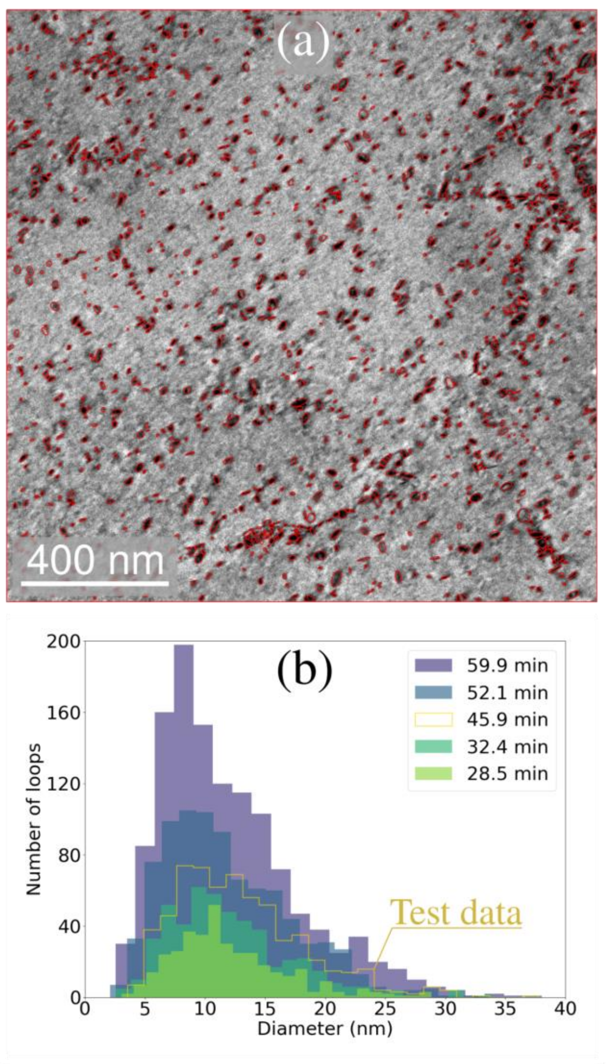

(2) Dataset: 3600 unique loops; 43835 + 10975 augmented loops

316L, 550 °C, 2 MeV Ni^{2+} ions, (2.8×10^{11} ions/cm^2.s)

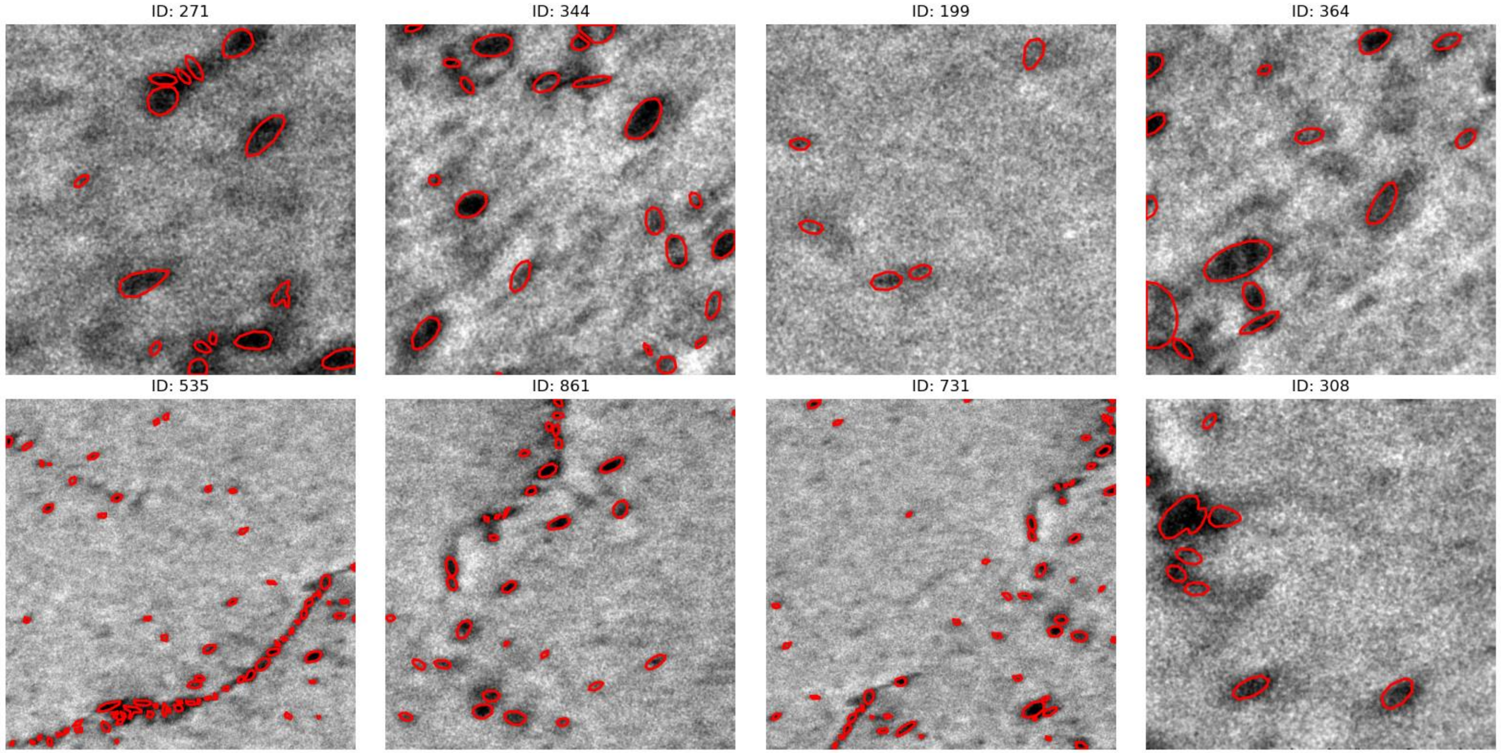

FOV = 800 nm (2%), 533 nm (28%), 400 nm (31%), 200 nm (39%)

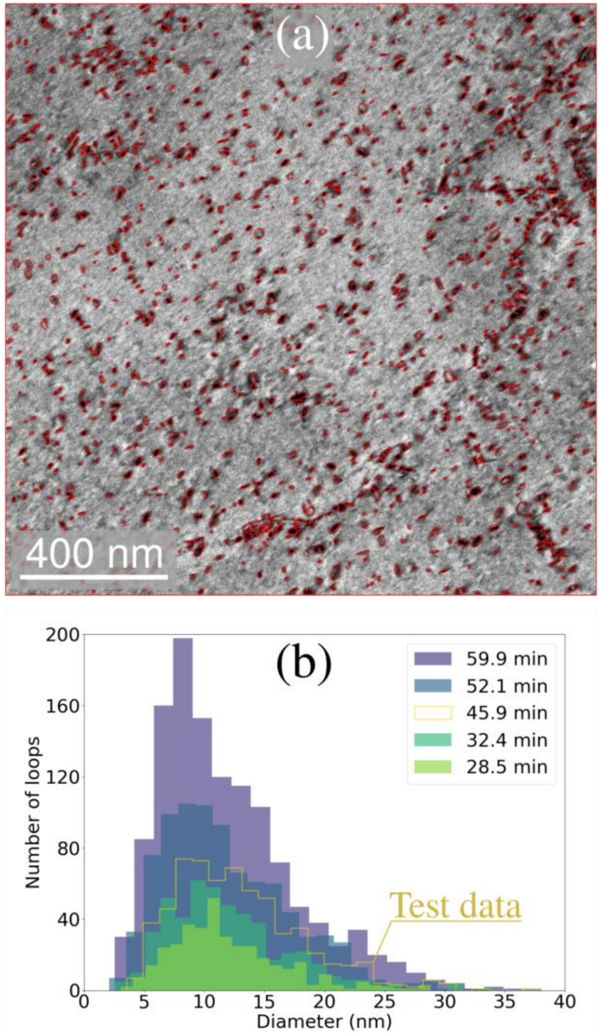

(2) Model training and evaluation

Salvador et al., 2026
Micron 201 103927

Backbone	Parameters (M)	FOV (nm)	Threshold	Run time (s)	Relative errors (%)				AP (%)	P_1	P_2
					F_{re}	N_{re}	D_{re}	$D_{m,re}$			
ResNeXt-101	89.46	200	0.8	11.0	1.01	-3.68	-10.03	-3.54	25.0	95.1	83.6
-	-	400	0.7	3.0	-8.10	-0.26	-22.81	-21.33	33.0	94.4	60.6
-	-	533	0.6	1.9	-9.88	2.59	-30.13	-30.57	36.6	88.0	49.8
Resnet-50	26.58	200	0.9	6.6	0.10	-0.15	-13.27	-6.01	19.6	97.2	81.4
-	-	400	0.8	1.9	0.94	-4.07	-15.71	-12.54	28.1	93.9	70.7
-	-	533	0.7	1.2	2.37	-1.77	-20.33	-19.20	33.0	92.9	63.2
Resnet-18	13.77	200	0.9	4.7	-19.79	-6.48	-13.71	-3.99	28.2	89.8	77.5
-	-	400	0.8	1.4	-16.62	-18.54	-14.32	-10.13	30.7	85.4	62.7
-	-	533	0.7	0.9	-13.02	-11.74	-21.09	-19.92	33.2	82.1	55.8

With:
F = foreground percentage
N = number of loops
S = loop sizes
(ellipses with D and Dm)

$$Y_{\text{re}} = \left(\frac{Y_{\text{pred}} - Y_{\text{gt}}}{Y_{\text{gt}}} \right) \times 100 \qquad (1)$$

$$A_i = \pi \cdot D \cdot D_m \qquad (3)$$

$$P_1 = 100 - 6 \left(\frac{1}{1+|F_{\text{re}}|} + \frac{1}{1+|N_{\text{re}}|} + \frac{4}{1+|S_{\text{re}}|} \right)^{-1} \qquad (2)$$

$$P_2 = A_{\text{tot}} = \langle N \rangle \cdot \pi \cdot \langle D \rangle \cdot \langle D_m \rangle \qquad (4)$$

(2) Results: use case A, ES1 alloy

Salvador et al., 2026
Micron 201 103927

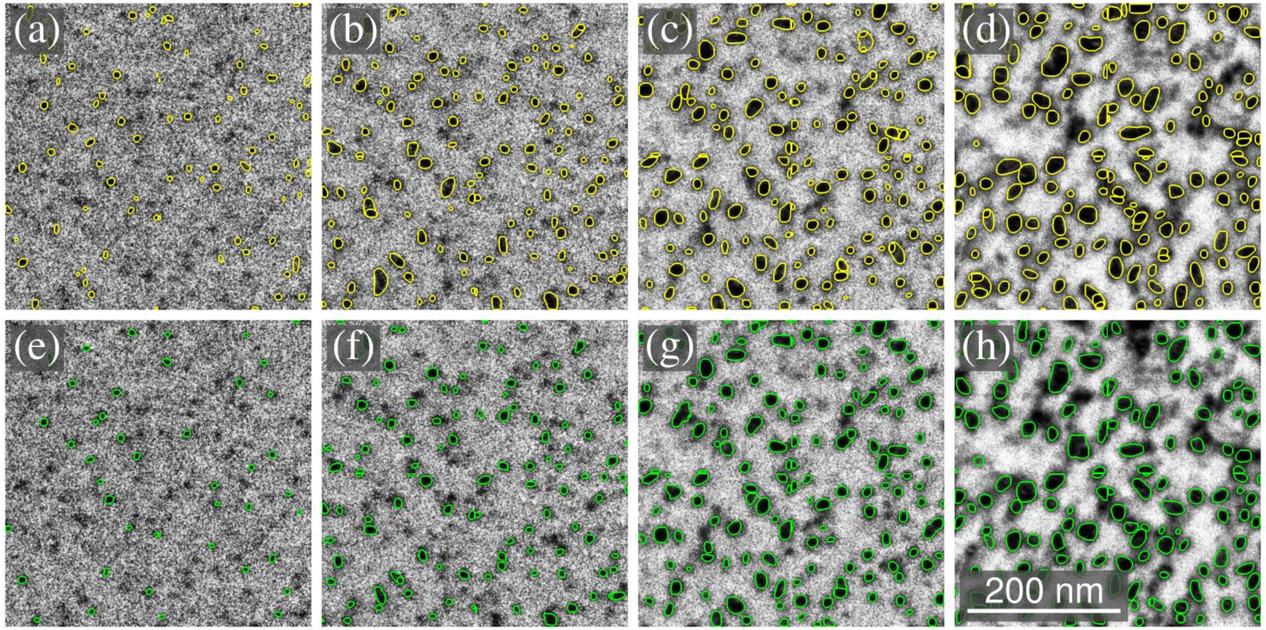

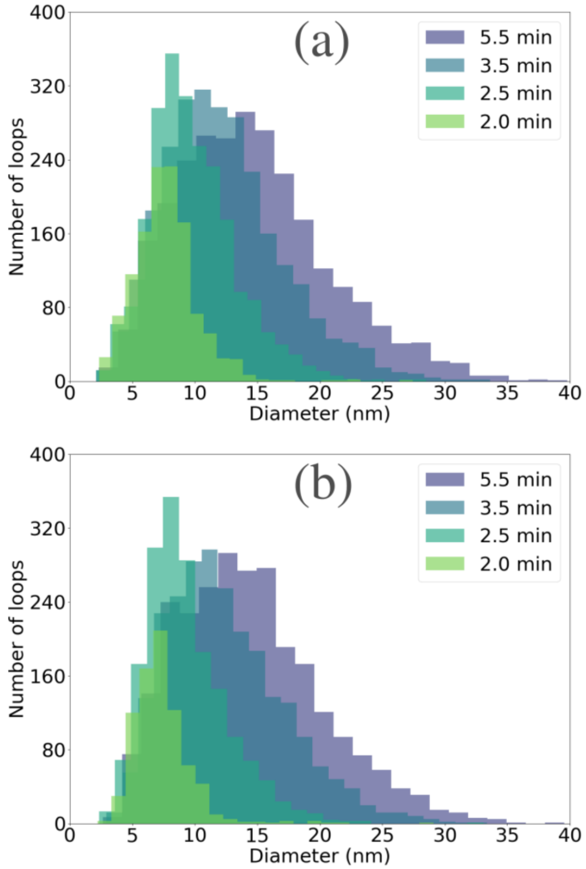

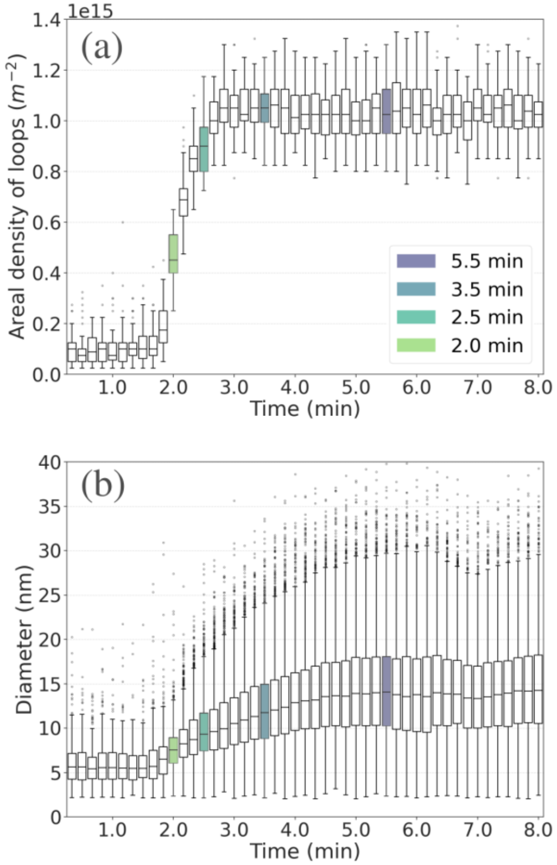

ES1 alloy: 16Cr-37Fe-13Mn-34Ni (at.%)
500 ℃, 2 MeV Ni^{2+} ions
(4.2 x 10^{12} ions/cm^2.s)

(2) Results: use case B, pure Cr (bcc)

Salvador et al., 2026
Micron 201 103927

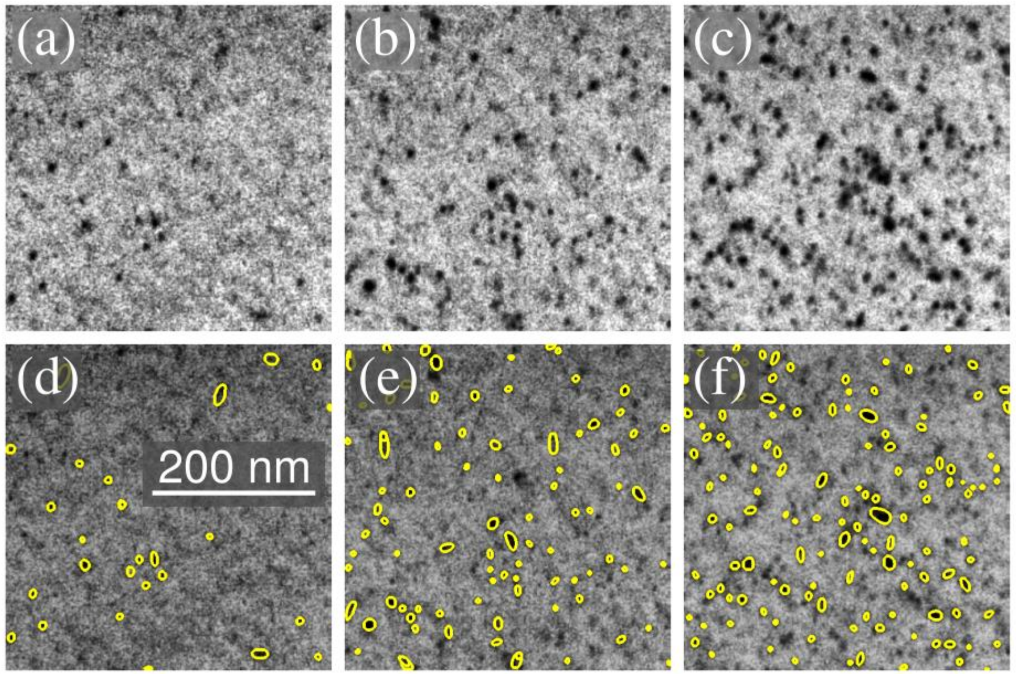

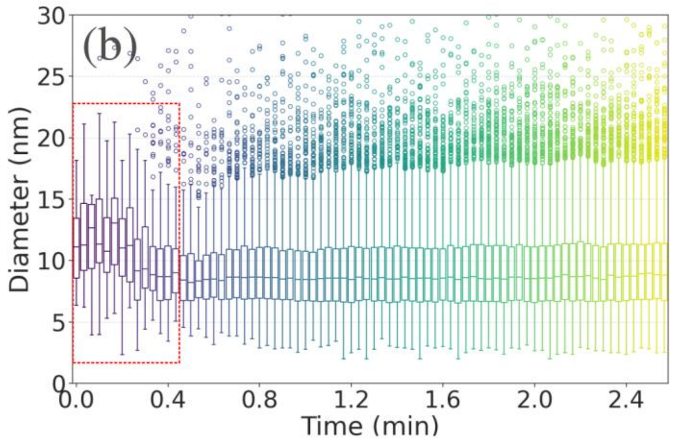

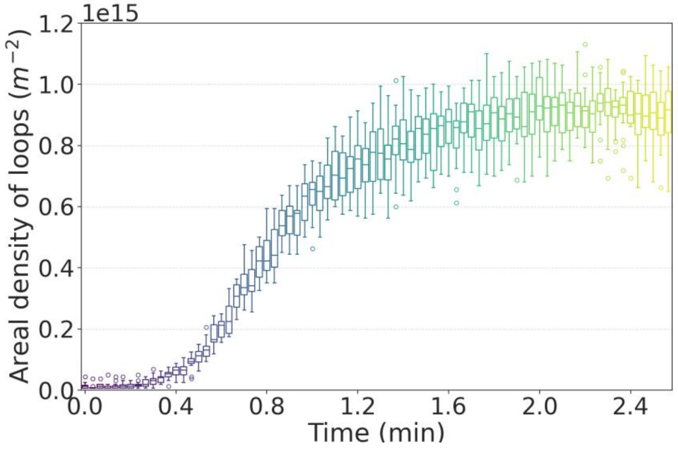

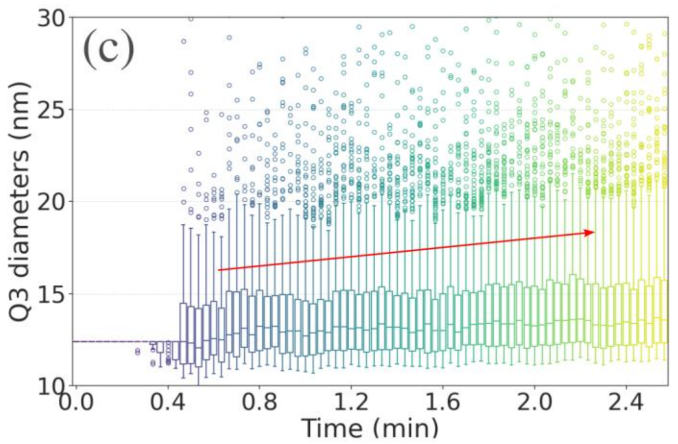

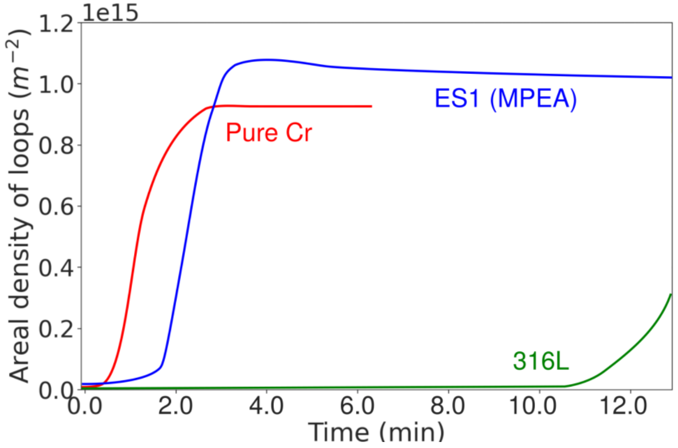

Pure Cr, 1024x1024 px
500 °C, 2 MeV Ni^{2+} ions
(4.2×10^{12} ions/cm^2.s)

(2) Results: use case C, particle tracking

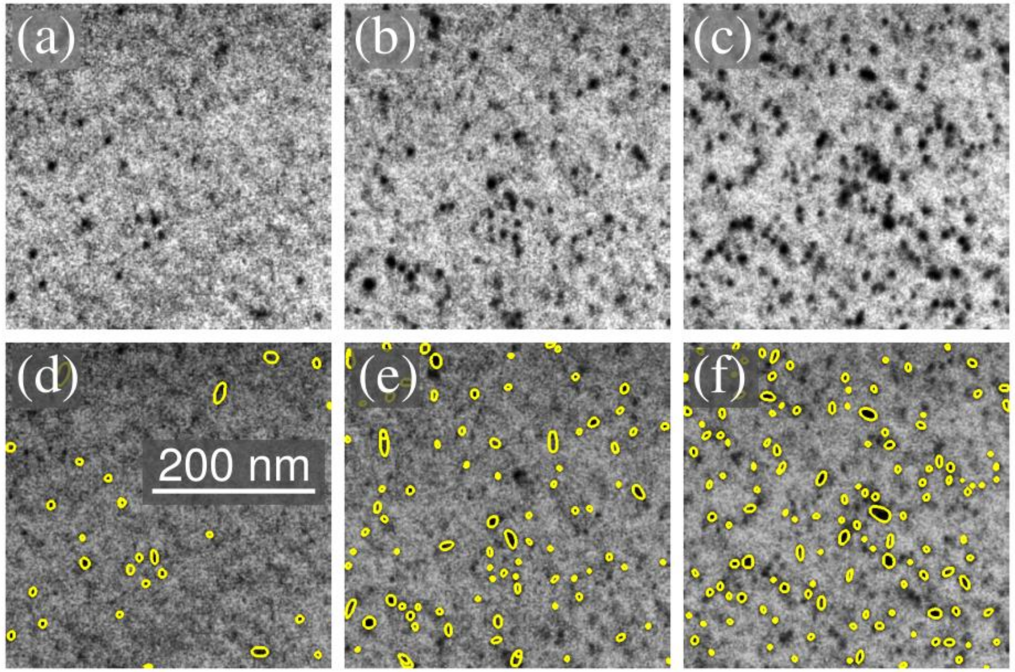

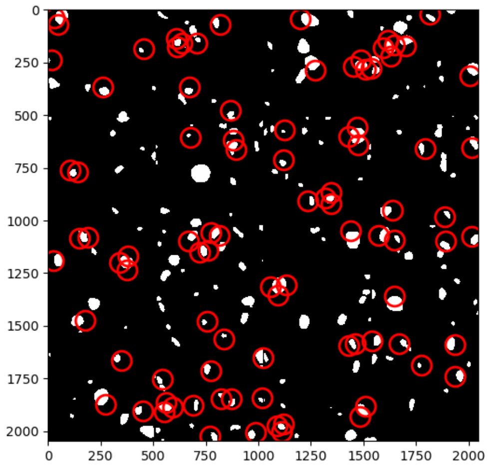

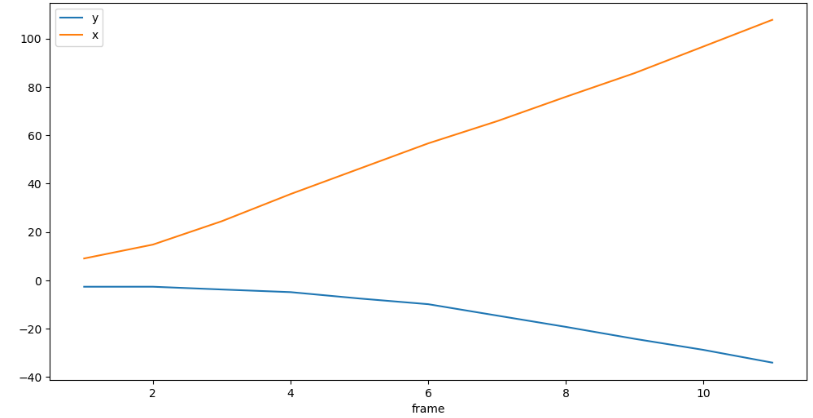

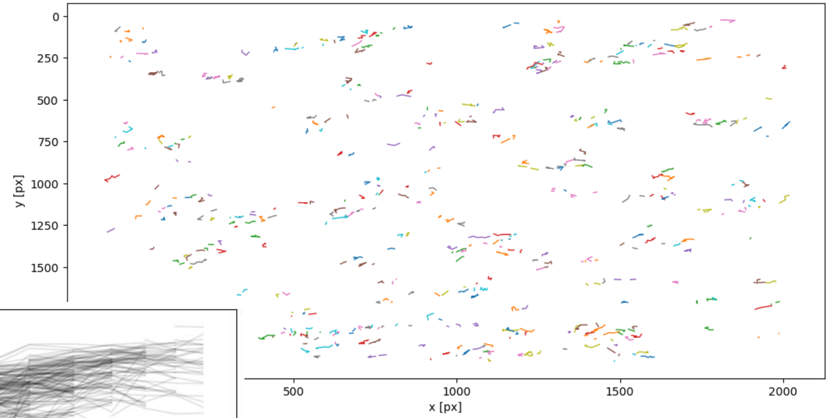

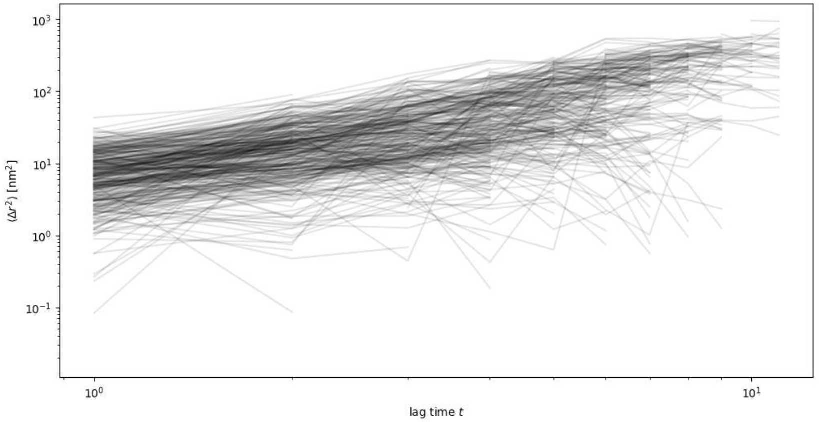

Integration with TrackPy

Loop re-indexation;

Calculation of: microscope stage drift, trajectories, mean-free path, growth-rate, etc.

soft-matter.github.io/trackpy

(2) Results: use case D, fine tuning (new dataset)

Base model detects 452 loops

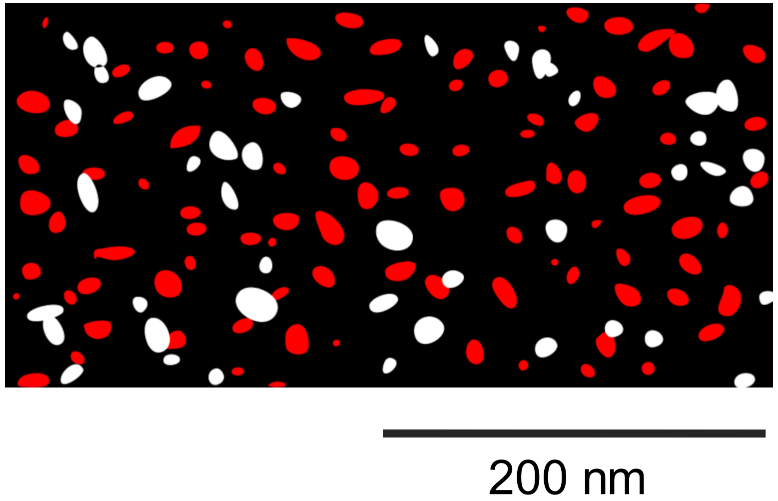

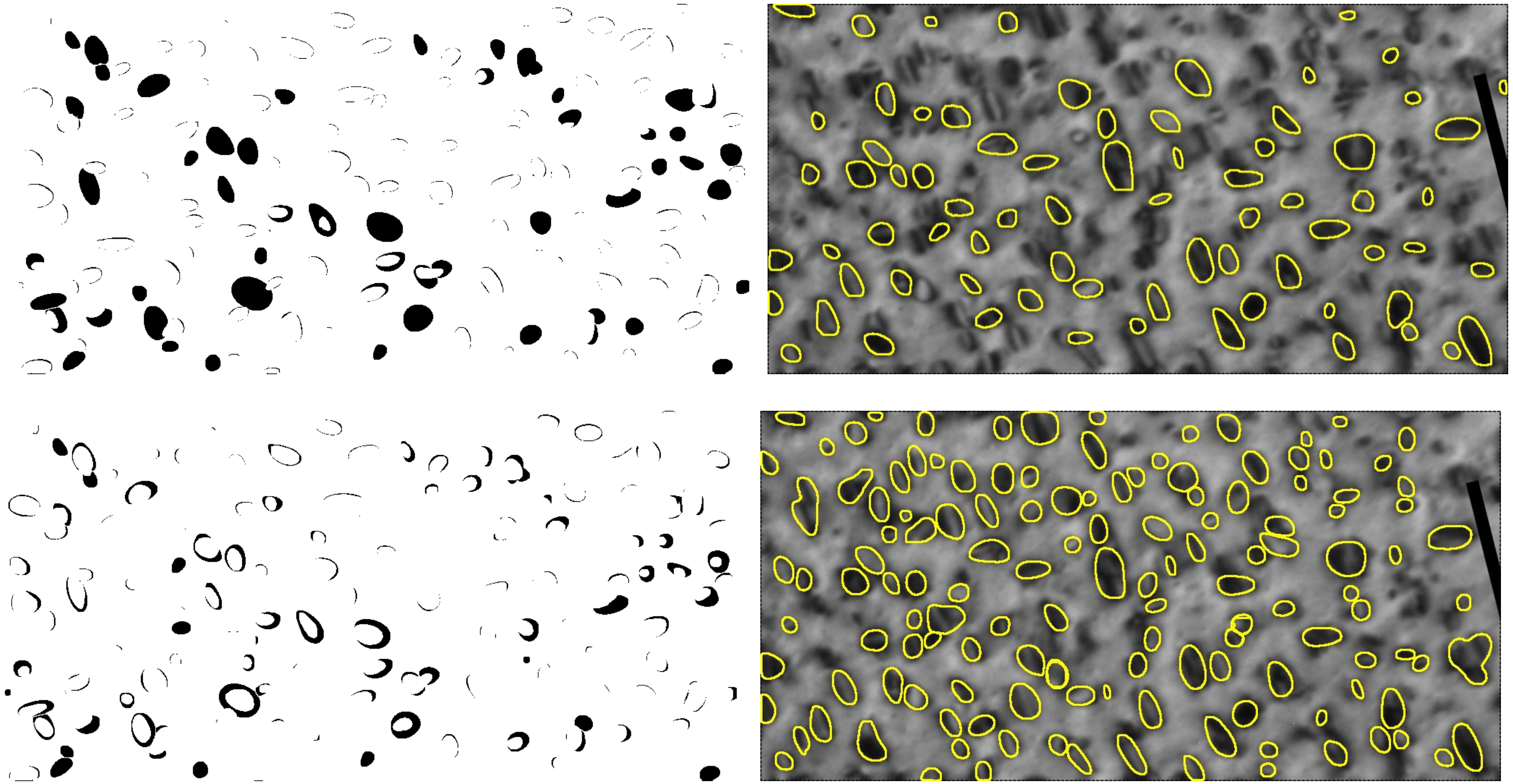

FT model detects 635 loops

New Ni-based alloy
Fine tuning is performed with only ⅙ of the original dataset

(3) Semantic models for dark-field segmentation

Ronnenberger et al., 2015
MICCAI pp. 234-241

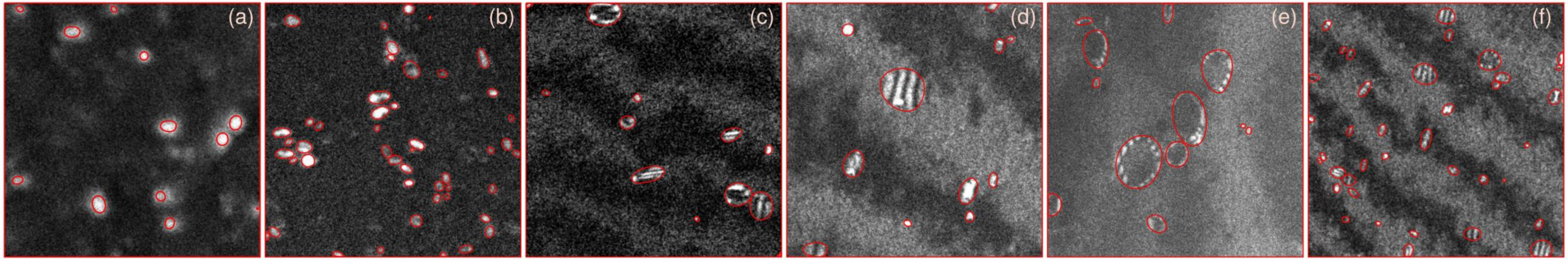

A detection-first strategy may fail when objects:

- lack a well-defined bounding box (e.g., topological or percolating structures),
- are defined by texture rather than shape
- are defined by the absence of contrast (e.g., pores)

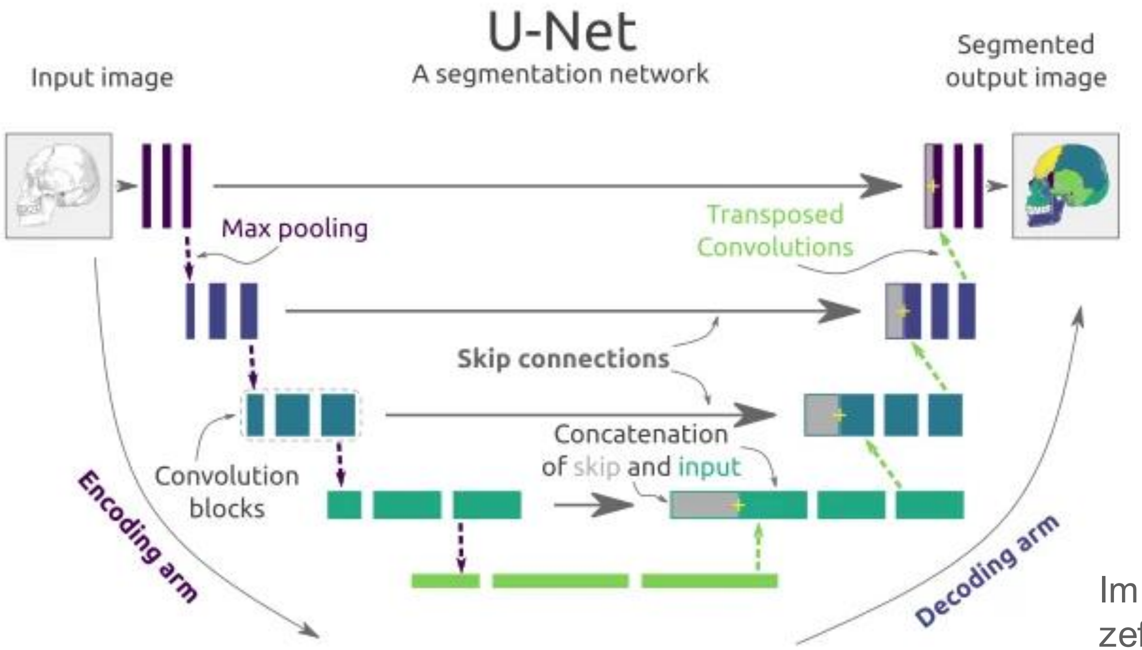

Image source: zefguides.com (2022)

(3) State-of-the-art: semantic models for dark-field segmentation

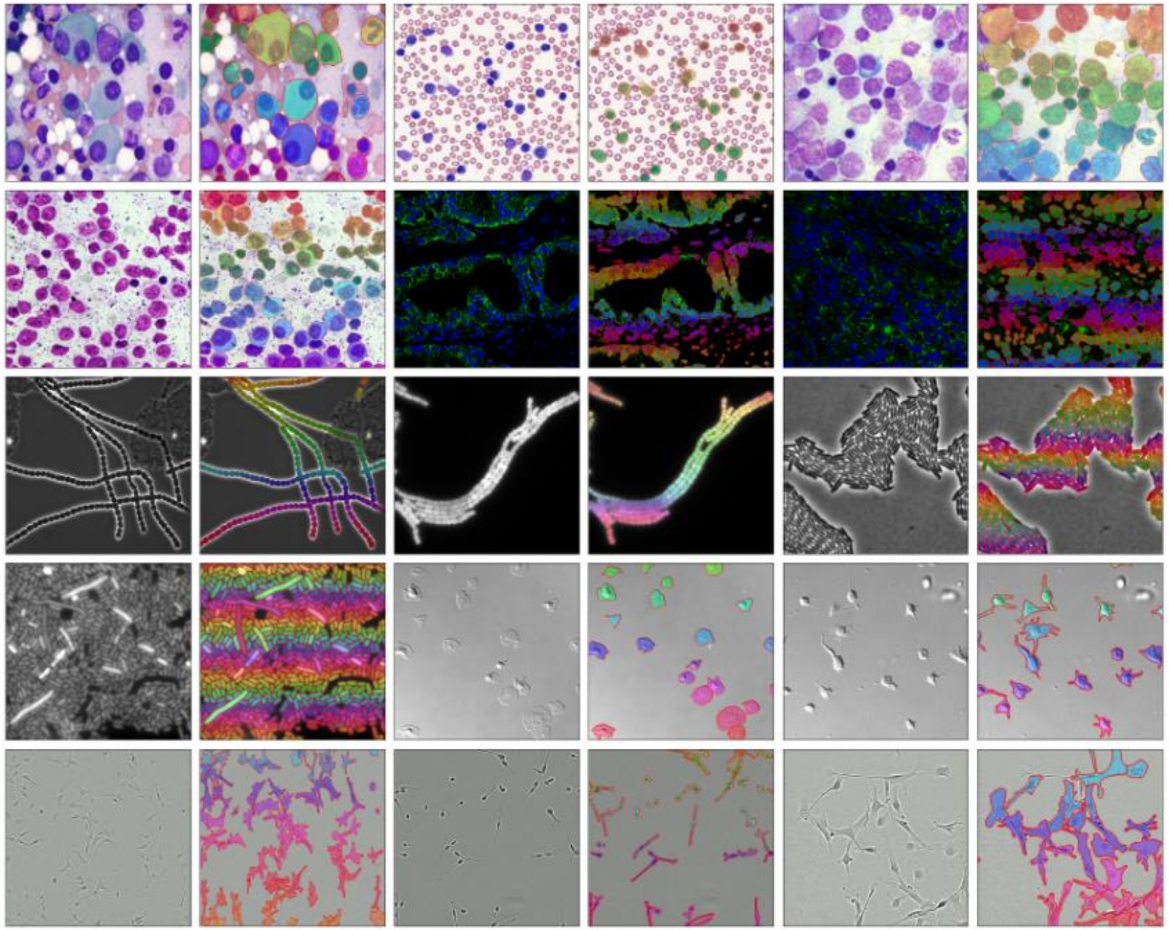

Figure 1: MEDIAR prediction results on *NeurIPS 2022 CellSeg Challenge* validation images. Our proposed method identifies the cell instances evenly well across different modalities.

ML Framework chosen: PyTorch

U-Net and U-Net++:
NASA's pre-trained microscopy models (pmm)
Pre-trained on MicroNet 1.0 (Stuckner et al. 2022), includes both SEM and TEM images;

MANet and SegForm: not implemented in pmm; (Pavel Iakubovskii) segmentation models (smp);

11,300 stars on GitHub; MIT License
Won the Open Cities AI Challenge (2019), MICCAI (2020), NeurIPS 2022 Cell Segmentation Challenge and the Severstal's Steel Defect Detection (2024);

Left-side image: Lee et al., (KAIST AI), 36th Conference on Neural Information Processing Systems (NeurIPS 2022); arXiv:2212.03465v1 [cs.CV], Dec. 2022

(3) Results: semantic models for dark-field segmentation

TABLE I. F1 (Dice) scores for different segmentation models and encoders

Model	Encoder	Train F1 (%)	Test F1 (%)
UNet	ResNet-50	87.3	69.6
UNet	EfficientNet-B3	94.0	71.9
UNet++	ResNet-50	80.5	69.7
UNet++	EfficientNet-B3	85.9	72.6
MANet	EfficientNet-B3	84.4	72.2
SegForm	EfficientNet-B0	83.4	73.8
SegForm	EfficientNet-B3	90.8	75.7
SegForm	EfficientNet-B5	86.5	**76.2**

For DF, Mask R-CNN F1 ~ 0.54

$$F1 = \frac{2\,TP}{2\,TP + FP + FN}.$$

TP = true positive; FP = false positive; FN = false negative;

Segformer
Xie et al., NeurIPS 2021.

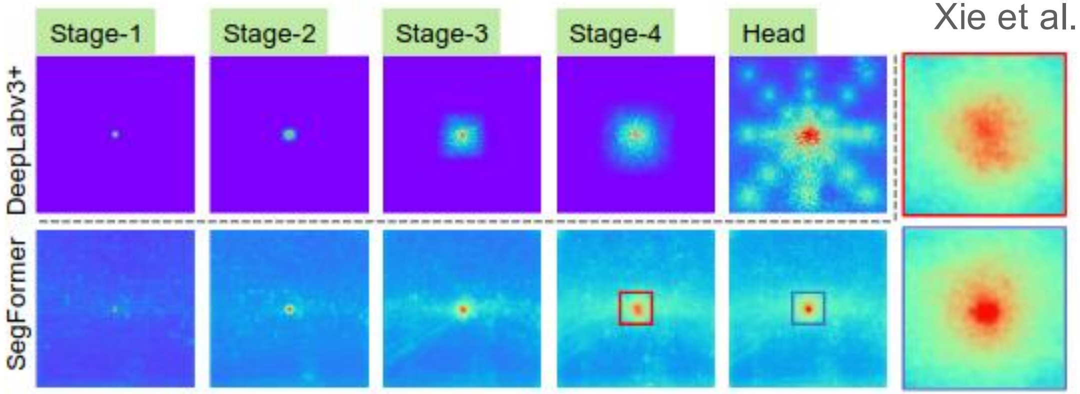

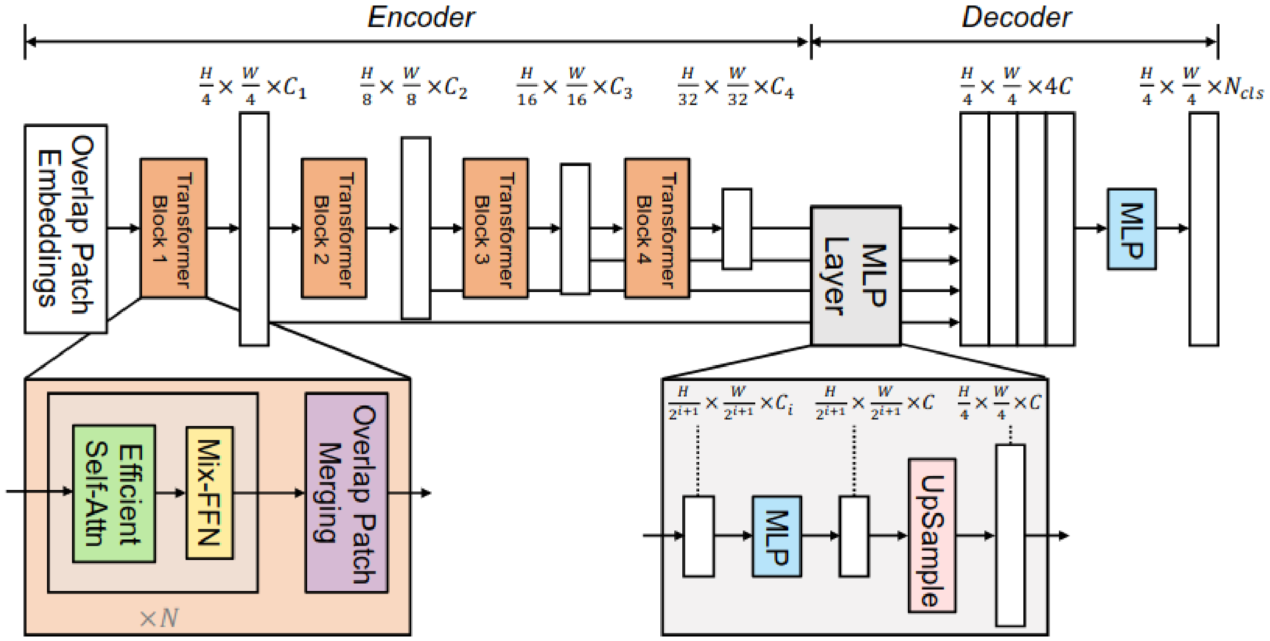

(3) Results: semantic models for dark-field segmentation

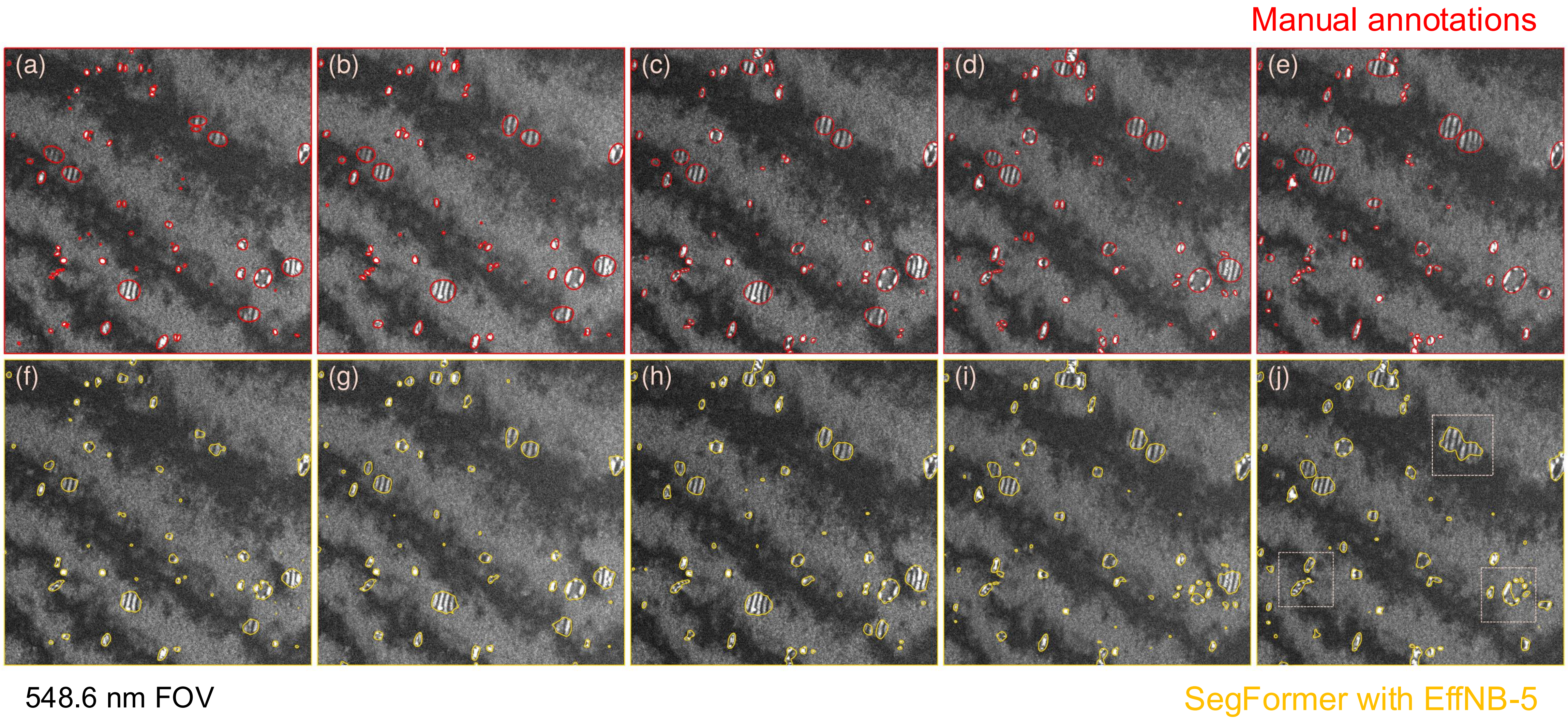

(3) Results: semantic models for dark-field segmentation

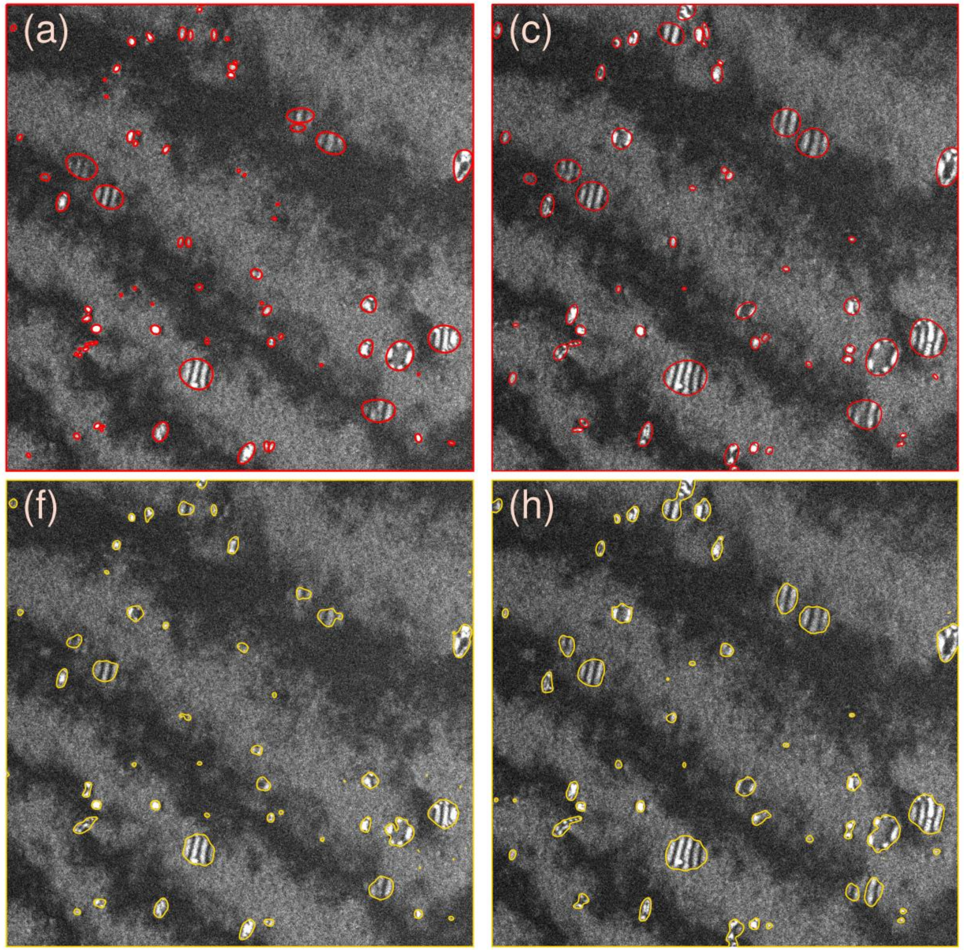

548.6 nm FOV

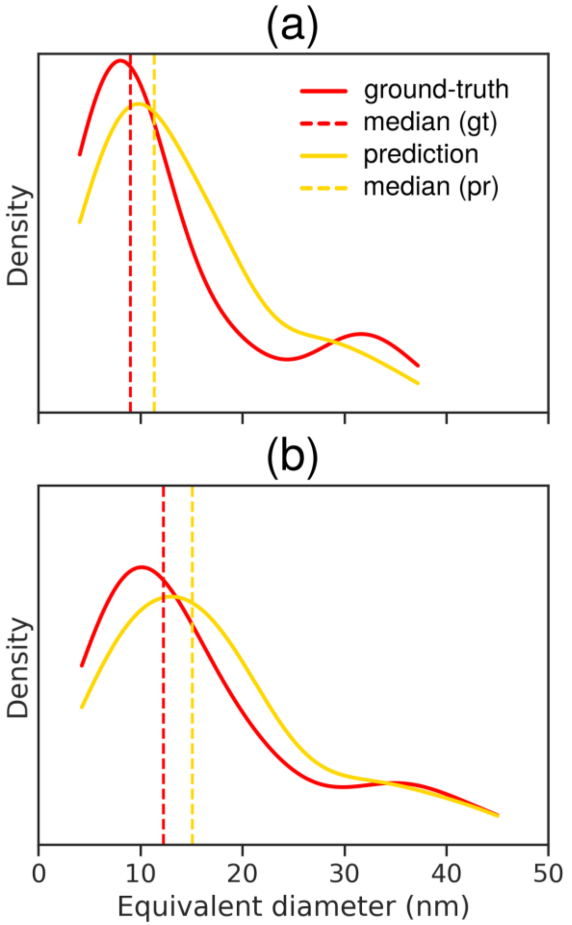

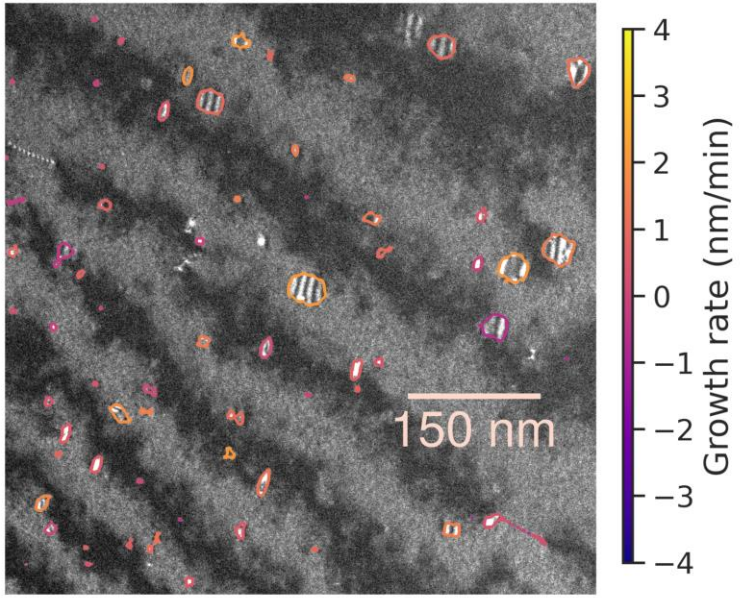

Conclusions & Perspectives

Classical segmentation, pure Cr

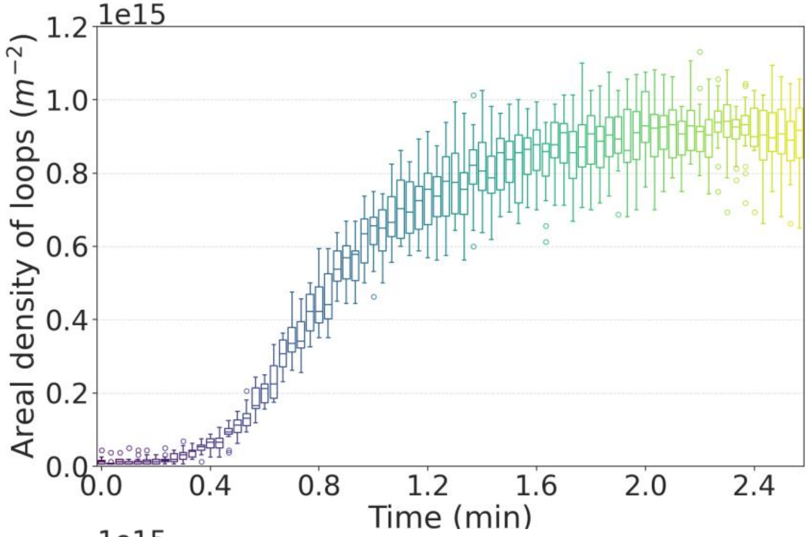

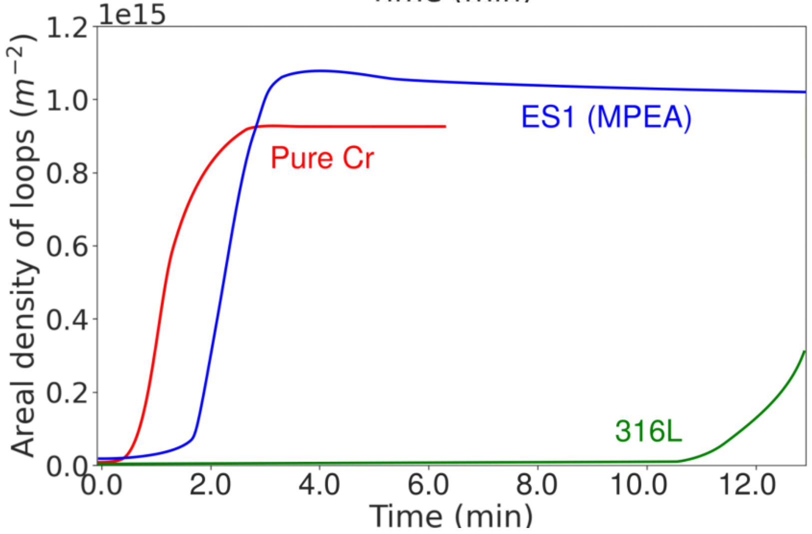

1) **DL in materials microscopy:**
- Big science platforms = big data;
- Latest models transitioned in ~3 years from CS to Mat. Sci.

1) **Image segmentation & data analysis**
- Near on-the-fly performance (4-5 fps);
- Robust comparison between different materials (same technique);
- Challenge: specialized versus “foundation” models.

1) **Transformers & other modern models**
- Semantic segmentation possible with an Improved receptive field;
- Challenge: computational cost scales with $O(N^2)$
- Multi-modal data: integrate orientation, diffraction, 4D-STEM, etc.

Thank you :) – if you have any ideas on using deep learning on a project, we would love to hear them:

camilo.fernandessalvador@cea.fr